

(12) INTERNATIONAL APPLICATION PUBLISHED UNDER THE PATENT COOPERATION TREATY (PCT)

(19) World Intellectual Property Organization

International Bureau



(10) International Publication Number

WO 2017/091474 A1

(43) International Publication Date

1 June 2017 (01.06.2017)

(51) International Patent Classification:

H01L 21/44 (2006.01)

(21) International Application Number:

PCT/US2016/062881

(22) International Filing Date:

18 November 2016 (18.11.2016)

(25) Filing Language:

English

(26) Publication Language:

English

(30) Priority Data:

14/757,124 23 November 2015 (23.11.2015) US

(71) Applicant (for all designated States except US): NANOTEK INSTRUMENTS, INC. [US/US]; 1240 McCook Ave, Dayton, Ohio 45404 (US).

(72) Inventors; and

(71) Applicants (for US only): ZHAMU, Aruna [CN/US]; Aruna Zhamu, 2749 Pekin Rd, Springboro, Ohio 45066 (US). JANG, Bor Z. [US/US]; Nanotek Instruments, 2301 E. Social Row Rd, Centerville, Ohio 45458 (US).

(74) Common Representative: JANG, Bor Z.; Nanotek Instruments, 2301 E. Social Row Rd, Centerville, Ohio 45458 (US).

(81) Designated States (unless otherwise indicated, for every kind of national protection available): AE, AG, AL, AM, AO, AT, AU, AZ, BA, BB, BG, BH, BN, BR, BW, BY,

BZ, CA, CH, CL, CN, CO, CR, CU, CZ, DE, DJ, DK, DM, DO, DZ, EC, EE, EG, ES, FI, GB, GD, GE, GH, GM, GT, HN, HR, HU, ID, IL, IN, IR, IS, JP, KE, KG, KN, KP, KR, KW, KZ, LA, LC, LK, LR, LS, LU, LY, MA, MD, ME, MG, MK, MN, MW, MX, MY, MZ, NA, NG, NI, NO, NZ, OM, PA, PE, PG, PH, PL, PT, QA, RO, RS, RU, RW, SA, SC, SD, SE, SG, SK, SL, SM, ST, SV, SY, TH, TJ, TM, TN, TR, TT, TZ, UA, UG, US, UZ, VC, VN, ZA, ZM, ZW.

(84) Designated States (unless otherwise indicated, for every kind of regional protection available): ARIPO (BW, GH, GM, KE, LR, LS, MW, MZ, NA, RW, SD, SL, ST, SZ, TZ, UG, ZM, ZW), Eurasian (AM, AZ, BY, KG, KZ, RU, TJ, TM), European (AL, AT, BE, BG, CH, CY, CZ, DE, DK, EE, ES, FI, FR, GB, GR, HR, HU, IE, IS, IT, LT, LU, LV, MC, MK, MT, NL, NO, PL, PT, RO, RS, SE, SI, SK, SM, TR), OAPI (BF, BJ, CF, CG, CI, CM, GA, GN, GQ, GW, KM, ML, MR, NE, SN, TD, TG).

Declarations under Rule 4.17:

- as to applicant's entitlement to apply for and be granted a patent (Rule 4.17(ii))
- as to the applicant's entitlement to claim the priority of the earlier application (Rule 4.17(iii))

Published:

- with international search report (Art. 21(3))

(54) Title: SUPERCAPACITOR ELECTRODES AND CELLS HAVING HIGH ACTIVE MASS LOADING

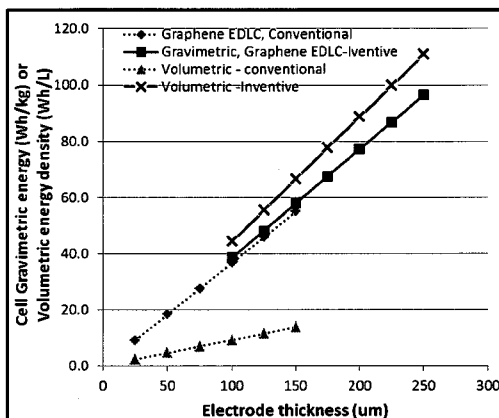


FIG. 11

(57) Abstract: A process for producing an electrode for a supercapacitor cell, said process comprising: (A) preparing a plurality of electrically conductive porous layers and a plurality of wet electrode layers composed of an electrode active material and an optional conductive additive mixed with a liquid or gel electrolyte, wherein the conductive porous layers contain interconnected conductive pathways and at least 80% by volume of pores; and (B) stacking and consolidating a desired number of the porous layers and a desired number of the wet electrode layers in an alternating sequence to form an electrode having a thickness no less than 100 μm (preferably greater than 200 μm , more preferably greater than 400 μm , further more preferably greater than 600 μm , and most preferably greater than 1,000 μm).

**Patent Application of
Aruna Zhamu and Bor Z. Jang
For
Supercapacitor Electrodes and Cells Having High Active Mass Loading**

CROSS-REFERENCE TO RELATED APPLICATIONS

The present application claims priority to US Patent Application No. 14/757,124, filed on November 23, 2015, which is hereby incorporated by reference.

FIELD OF THE INVENTION

The present invention relates generally to the field of supercapacitors or ultracapacitors, and more particularly to the production processes for supercapacitor electrodes and cells.

BACKGROUND OF THE INVENTION

Electrochemical capacitors (ECs), also known as ultracapacitors or supercapacitors, are being considered for uses in hybrid electric vehicles (EVs) where they can supplement a battery used in an electric car to provide bursts of power needed for rapid acceleration, the biggest technical hurdle to making battery-powered cars commercially viable. A battery would still be used for cruising, but supercapacitors (with their ability to release energy much more quickly than batteries) would kick in whenever the car needs to accelerate for merging, passing, emergency maneuvers, and hill climbing. The EC must also store sufficient energy to provide an acceptable driving range. To be cost-, volume-, and weight-effective compared to additional battery capacity they must combine adequate energy densities (volumetric and gravimetric) and power densities with long cycle life, and meet cost targets as well.

ECs are also gaining acceptance in the electronics industry as system designers become familiar with their attributes and benefits. ECs were originally developed to provide large bursts of driving energy for orbital lasers. In complementary metal oxide semiconductor (CMOS) memory backup applications, for instance, a one-Farad EC having a volume of only one-half cubic inch can replace nickel-cadmium or lithium batteries and provide backup power for months. For a given applied voltage, the stored energy in an EC associated with a given charge is half that storable in a corresponding battery system for passage of the same charge. Nevertheless, ECs are extremely attractive power sources. Compared with batteries, they require no maintenance, offer much higher cycle-life, require a very simple charging circuit, experience no “memory effect,” and are generally much safer. Physical rather than chemical energy storage is

the key reason for their safe operation and extraordinarily high cycle-life. Perhaps most importantly, capacitors offer higher power density than batteries.

The high capacitance density of an EC relative to conventional capacitors (10 to 100 times greater than conventional capacitors) derives from using porous electrodes to create a large effective "plate area" and from storing energy in the diffuse double layer. This double layer, created naturally at a solid-electrolyte interface when voltage is imposed, has a thickness of only about 1 nm, thus forming an extremely small effective "plate separation." Such a supercapacitor is commonly referred to as an electric double layer capacitor (EDLC). The double layer capacitor is based on a high surface area electrode material, such as activated carbon, immersed in a liquid electrolyte. A polarized double layer is formed at electrode-electrolyte interfaces providing high capacitance. This implies that the specific capacitance of a supercapacitor is directly proportional to the specific surface area of the electrode material. However, this surface area must be accessible by electrolyte and the resulting interfacial zones must be sufficiently large to accommodate the so-called electric double-layer charges.

In some ECs, stored energy is further augmented by *pseudo-capacitance* effects, occurring again at the solid-electrolyte interface due to such electrochemical phenomena as the redox charge transfer.

However, there are several serious technical issues associated with current state-of-the-art ECs or supercapacitors:

(1) Experience with ECs based on activated carbon electrodes shows that the experimentally measured capacitance is always much lower than the geometrical capacitance calculated from the measured surface area and the width of the dipole layer. For very high surface area carbons, typically only about 10-20 percent of the "theoretical" capacitance was observed. This disappointing performance is related to the presence of micro-pores (< 2 nm, mostly < 1 nm) and ascribed to inaccessibility of some pores by the electrolyte, wetting deficiencies, and/or the inability of a double layer to form successfully in pores in which the oppositely charged surfaces are less than about 1 nm apart. In activated carbons, depending on the source of the carbon and the heat treatment temperature, a surprising amount of surfaces can be in the form of such micro-pores.

(2) Despite the high gravimetric capacitances at the electrode level (based on active material weights alone) as frequently claimed in open literature and patent documents, these electrodes unfortunately fail to provide energy storage devices with high capacities at the supercapacitor cell or pack level (based on the total cell weight or pack weight). This is due to the notion that, in these reports, the actual mass loadings of the electrodes and the apparent densities for the active materials are too low. In most cases, the active material mass loadings of the electrodes (areal density) is significantly lower than 10 mg/cm^2 (areal density = the amount of active materials per electrode cross-sectional area along the electrode thickness direction) and the apparent volume density or tap density of the active material is typically less than 0.75 g/cm^3 (more typically less than 0.5 g/cm^3 and most typically less than 0.3 g/cm^3) even for relatively large particles of activated carbon.

The low mass loading is primarily due to the inability to obtain thicker electrodes (thicker than $100\text{--}200 \mu\text{m}$) using the conventional slurry coating procedure. This is not a trivial task as one might think, and in reality the electrode thickness is not a design parameter that can be arbitrarily and freely varied for the purpose of optimizing the cell performance. Contrarily, thicker samples tend to become extremely brittle or of poor structural integrity and would also require the use of large amounts of binder resin. These problems are particularly acute for graphene material-based electrodes. It has not been previously possible to produce graphene-based electrodes that are thicker than $150 \mu\text{m}$ and remain highly porous with pores remaining fully accessible to liquid electrolyte. The low areal densities and low volume densities (related to thin electrodes and poor packing density) result in relatively low volumetric capacitances and low volumetric energy density of the supercapacitor cells.

With the growing demand for more compact and portable energy storage systems, there is keen interest to increase the utilization of the volume of the energy storage devices. Novel electrode materials and designs that enable high volumetric capacitances and high mass loadings are essential to achieving improved cell volumetric capacitances and energy densities.

(3) During the past decade, much work has been conducted to develop electrode materials with increased volumetric capacitances utilizing porous carbon-based materials, such as graphene,

carbon nanotube-based composites, porous graphite oxide, and porous meso carbon. Although these experimental supercapacitors featuring such electrode materials can be charged and discharged at high rates and also exhibit large volumetric electrode capacitances (100 to 200 F/cm³ in most cases, based on the electrode volume), their typical active mass loading of <1 mg/cm², tap density of < 0.2 g/cm³, and electrode thicknesses of up to tens of micrometers (<< 100 µm) are still significantly lower than those used in most commercially available electrochemical capacitors (i.e. 10 mg/cm², 100–200 µm), which results in energy storage devices with relatively low areal and volumetric capacitances and low volumetric energy densities.

(4) For graphene-based supercapacitors, there are additional problems that remain to be solved, explained below:

Nano graphene materials have recently been found to exhibit exceptionally high thermal conductivity, high electrical conductivity, and high strength. Another outstanding characteristic of graphene is its exceptionally high specific surface area. A single graphene sheet provides a specific external surface area of approximately 2,675 m²/g (that is accessible by liquid electrolyte), as opposed to the exterior surface area of approximately 1,300 m²/g provided by a corresponding single-wall CNT (interior surface not accessible by electrolyte). The electrical conductivity of graphene is slightly higher than that of CNTs.

The instant applicants (A. Zhamu and B. Z. Jang) and their colleagues were the first to investigate graphene- and other nano graphite-based nano materials for supercapacitor application [Please see Refs.1-5 below; the 1st patent application was submitted in 2006 and issued in 2009]. After 2008, researchers began to realize the significance of nano graphene materials for supercapacitor applications.

List of References:

1. Lulu Song, A. Zhamu, Jiusheng Guo, and B. Z. Jang "Nano-scaled Graphene Plate Nanocomposites for Supercapacitor Electrodes" US Pat. No. 7,623,340 (11/24/2009).

2. Aruna Zhamu and Bor Z. Jang, "Process for Producing Nano-scaled Graphene Platelet Nanocomposite Electrodes for Supercapacitors," U.S. Patent Appl. No. 11/906,786 (10/04/2007).
3. Aruna Zhamu and Bor Z. Jang, "Graphite-Carbon Composite Electrodes for Supercapacitors" US Pat. Appl. No. 11/895,657 (08/27/2007).
4. Aruna Zhamu and Bor Z. Jang, "Method of Producing Graphite-Carbon Composite Electrodes for Supercapacitors" US Pat. Appl. No. 11/895,588 (08/27/2007).
5. Aruna Zhamu and Bor Z. Jang, "Graphene Nanocomposites for Electrochemical cell Electrodes," U.S. Patent Appl. No. 12/220,651 (07/28/2008).

However, individual nano graphene sheets have a great tendency to re-stack themselves, effectively reducing the specific surface areas that are accessible by the electrolyte in a supercapacitor electrode. The significance of this graphene sheet overlap issue may be illustrated as follows: For a nano graphene platelet with dimensions of l (length) x w (width) x t (thickness) and density ρ , the estimated surface area per unit mass is $S/m = (2/\rho) (1/l + 1/w + 1/t)$. With $\rho \approx 2.2 \text{ g/cm}^3$, $l = 100 \text{ nm}$, $w = 100 \text{ nm}$, and $t = 0.34 \text{ nm}$ (single layer), we have an impressive S/m value of $2,675 \text{ m}^2/\text{g}$, which is much greater than that of most commercially available carbon black or activated carbon materials used in the state-of-the-art supercapacitor. If two single-layer graphene sheets stack to form a double-layer graphene, the specific surface area is reduced to $1,345 \text{ m}^2/\text{g}$. For a three-layer graphene, $t=1 \text{ nm}$, we have $S/m = 906 \text{ m}^2/\text{g}$. If more layers are stacked together, the specific surface area would be further significantly reduced.

These calculations suggest that it is critically important to find a way to prevent individual graphene sheets to re-stack and, even if they partially re-stack, the resulting multi-layer structure would still have inter-layer pores of adequate sizes. These pores must be sufficiently large to allow for accessibility by the electrolyte and to enable the formation of electric double-layer charges, which typically require a pore size of at least 1 nm, more preferably at least 2 nm. However, these pores or inter-graphene spacings must also be sufficiently small to ensure a large tap density (electrode mass per unit volume). Unfortunately, the typical tap density of graphene-based electrode is less than 0.3 g/cm^3 , and most typically <<

0.1 g/cm³. To a great extent, the requirement to have large pore sizes and high porosity level and the requirement to have a high tap density are considered mutually exclusive in supercapacitors.

Another major technical barrier to using graphene sheets as a supercapacitor electrode active material is the challenge of depositing a thick active material layer onto the surface of a solid current collector (e.g. Al foil) using the conventional graphene-solvent slurry coating procedure. In such an electrode, the graphene electrode typically requires a large amount of a binder resin (hence, significantly reduced active material proportion vs. non-active or overhead materials/components). In addition, any electrode prepared in this manner that is thicker than 50 μ m is brittle and weak, having a great tendency to delaminate and micro-crack. These characteristics have made the supercapacitor electrode thickness not a design parameter, but a manufacturing-limited feature. A supercapacitor designer cannot freely increase the electrode thickness. There has been no effective solution to these problems.

Therefore, there is a clear and urgent need for supercapacitor cells and electrodes that have a high active material mass loading (high areal density), active materials with a high apparent density (high tap density), high electrode thickness with structural integrity and without significantly decreased electron and ion transport rates (e.g. without large electron transport resistance), high volumetric capacitance, and high volumetric energy density. For graphene-based electrodes, one must also overcome problems such as re-stacking of graphene sheets, the demand for large proportion of a binder resin, and difficulty in producing thick graphene electrode layers.

SUMMARY OF THE INVENTION

The present invention provides a process for producing supercapacitor electrodes and further for producing the supercapacitor cell having a high active material mass loading, exceptionally low overhead (ancillary component) weight and volume (relative to the active material mass and volume), high volumetric capacitance, and unprecedentedly high volumetric energy density. This process is highly scalable, amenable to mass production of supercapacitor electrodes and cells in a cost-effective manner.

In one embodiment, the invented process for producing a supercapacitor cell comprises:

- (a) Preparing a plurality of electrically conductive porous layers (e.g. highly porous Ni foam), a plurality of wet anode layers of an anode active material (e.g. activated carbon particles and/or graphene sheets) and an optional conductive additive mixed with a first liquid or gel electrolyte, and a plurality of wet cathode layers of a cathode active material and an optional conductive additive mixed with a second liquid or gel electrolyte, wherein the conductive porous layers contain interconnected conductive pathways and at least 80% by volume of pores;
- (b) Stacking and consolidating a desired number of the porous layers and a desired number of the wet anode layers preferably in an alternating sequence to form an anode electrode having a thickness no less than 100 μm (preferably $> 200 \mu\text{m}$, more preferably $> 500 \mu\text{m}$; no theoretical thickness limit, practical limit is 1 m);
- (c) Placing a porous separator layer in contact with the anode electrode;
- (d) Stacking and consolidating a desired number of the porous layers and a desired number of the wet cathode layers in an alternating sequence to form a cathode electrode in contact with the porous separator, wherein the cathode electrode has a thickness no less than 100 μm ; wherein step (d) is conducted before or after step (b); and
- (e) Assembling and sealing the anode electrode, porous separator, and cathode electrode in a housing to produce the supercapacitor cell;

wherein the anode electrode and/or said cathode electrode has a material mass loading no less than 7 mg/cm^2 (preferably higher than 10 mg/cm^2 , more preferably higher than 20 mg/cm^2 , and further more preferably higher than 30 mg/cm^2 , and most preferably higher than 50 mg/cm^2).

In certain embodiments, the anode active material and/or said cathode active material contains multiple particles of a carbon material and/or multiple graphene sheets, wherein said multiple graphene sheets contain single-layer graphene or few-layer graphene each having from 1 to 10 graphene planes and said multiple particles of carbon material have a specific surface area no less than 500 m^2/g when measured in a dried state.

In this supercapacitor production process, steps (a) and (b) combined or steps (a) and (d) combined each essentially constitute a production process for an electrode (an anode or cathode).

Hence, another embodiment of the present invention is a process for producing an electrode for a supercapacitor cell, the process comprising: (A) preparing a plurality of electrically conductive porous layers and a plurality of wet electrode layers each composed of an electrode active material and an optional conductive additive mixed with a liquid or gel electrolyte, wherein the conductive porous layers contain interconnected conductive pathways and at least 80% by volume of pores; and (B) stacking and consolidating a desired number of the porous layers and a desired number of the wet electrode layers in an alternating sequence to form an electrode having a thickness no less than 100 μm . Again, the electrode active material may be selected from multiple particles of a carbon material and/or multiple graphene sheets, wherein said multiple graphene sheets contain single-layer graphene or few-layer graphene each having from 1 to 10 graphene planes and said multiple particles of carbon material have a specific surface area no less than 500 m^2/g when measured in a dried state.

The electrically conductive porous layers in the anode and those in the cathode can be made of the same material or different materials. Each layer contains interconnected 2D or 3D network of electron-conducting paths as a cathode current collector or anode current collector having pores to accommodate liquid or gel electrolyte and a cathode active material or an anode active material. The conductive porous layer has a thickness no less than 100 μm (preferably greater than 200 μm , more preferably greater than 300 μm , further preferably greater than 400 μm , still more preferably greater than 500 μm , and most preferably up to 5,000 μm or 5 mm (actually, there is no limitation on the porous layer thickness or final electrode thickness). The conductive porous layer preferably has at least 70% by volume of pores (more preferably at least 80% porosity, still more preferably at least 90%, and most preferably at least 95%).

In some embodiments, the anode active material and/or the cathode active material contains multiple particles of a carbon material and/or multiple graphene sheets, wherein the multiple graphene sheets contain single-layer graphene or few-layer graphene (each having from 1 to 10 graphene planes) and the multiple particles of carbon material have a specific surface area no less than 500 m^2/g (preferably $> 1,000 \text{ m}^2/\text{g}$, more preferably $> 1,500 \text{ m}^2/\text{g}$, further more preferably $> 2,000 \text{ m}^2/\text{g}$, still more preferably $> 2,500 \text{ m}^2/\text{g}$, and most preferably more preferably $> 3,000 \text{ m}^2/\text{g}$) when measured in a dried state (the practical limit is 3,500 m^2/g for carbon-based

materials). In the final electrode, the anode active material or the cathode active material constitutes an electrode active material loading no less than 7 mg/cm^2 (preferably higher than 10 mg/cm^2 , more preferably higher than 20 mg/cm^2 , further more preferably higher than 30 mg/cm^2 , still more preferably higher than 50 mg/cm^2 , and most preferably higher less than 100 mg/cm^2) in the anode or the cathode. Such high mass loadings have not been achievable by any previously conceived methods.

The electrically conductive porous layer herein refers to a structure that contains a high pore volume (> 70% or more) and an interconnected network of electron-conducting paths. This can be, for instance, end-connected 2D mats, webs, chicken wire-like metal screens, etc. As illustrated in Fig. 3(A)-(D), this can also be metal foam, conductive polymer foam, graphite foam, carbon foam, or graphene foam, etc., wherein pore walls contain conductive materials. The pore volume (e.g. > 70%) of a conductive porous layer (serving as a current collector) is a critically important requirement to ensure a large proportion of active materials being accommodated in the current collector. Based on this criterion, conventional paper or textiles made of natural and/or synthetic fibers do not meet this requirement since they do not have a sufficient amount of properly sized pores.

The pore sizes in the conductive porous layers are preferably in the range from 10 nm to $50 \mu\text{m}$, more preferably from 100 nm to $20 \mu\text{m}$, further preferably from 500 nm to $10 \mu\text{m}$, and most preferably from 1 μm to 5 μm . These pore size ranges are designed to accommodate graphene sheets, which are typically from 10 nm to $50 \mu\text{m}$ in length/width and most typically from 100 nm to $20 \mu\text{m}$, further typically from 200 nm to $10 \mu\text{m}$, and most typically from 0.5 μm to 5 μm . More significantly, however, since all active material particles (e.g. graphene sheets, carbon particles, etc.) are, on average, within a distance of $25 \mu\text{m}$ from a pore wall in the 3D foam structure, electrons (charges) can be readily collected from the electric double layers near the active material-electrolyte interface. This is in contrast to the notion that some electrons in the conventional thick electrode of prior art supercapacitors (e.g. wherein an activated carbon layer > $100 \mu\text{m}$ in thickness is coated onto a surface of a solid Al foil current collector 12 μm thick) must travel at least $100 \mu\text{m}$ to get collected by a current collector (meaning a larger internal resistance and reduced ability to deliver a higher power).

In general, the wet anode layer and the wet cathode layer are identical in composition in a symmetric supercapacitor (e.g. an electric double layer capacitor, EDLC, or redox pseudo-capacitor), but they can be different in composition. The liquid electrolytes can contain an aqueous liquid, organic liquid, ionic liquid (ionic salt having a melting temperature lower than 100°C, preferably lower than room temperature, 25°C), or mixture of an ionic liquid and an organic liquid at a ratio from 1/100 to 100/1. The organic liquid is desirable, but the ionic liquid is preferred.

A supercapacitor active material is a material responsible for storing charges via the nearby electric double layers or via the redox mechanism in the supercapacitor cell. As an active material, the carbon material may be selected from activated carbon, activated meso-carbon micro beads (activated MCMBs), activated graphite, activated or chemically etched carbon black, activated hard carbon, activated soft carbon, carbon nanotube, carbon nano-fiber, activated carbon fiber, activated graphite fiber, exfoliated graphite worms, activated graphite worms, activated expanded graphite flakes, or a combination thereof.

In a preferred embodiment, the first and/or second conductive porous layer has a thickness no less than 200 μm , has at least 85% by volume of pores (prior to impregnation of the wet electrode active material mixture), and/or the electrode active material loading is no less than 10 mg/cm^2 . Preferably, the active material in the two electrodes (anode and cathode) combined occupies at least 30% by weight or by volume of the entire supercapacitor cell. This weight or volume proportion of the active material is preferably no less than 40%, further preferably no less than 50%, and more preferably no less than 60%. These have not been possible with conventional supercapacitors.

In a further preferred embodiment, the first and/or second conductive porous layer structure has a thickness no less than 300 μm , has at least 90% by volume of pores, and/or the electrode active material loading is no less than 15 mg/cm^2 (there is no theoretical upper limit to this areal density of active material mass achievable with the presently invented method).

In a more preferred embodiment, the first and/or second conductive porous layer structure has a thickness no less than 400 μm , has at least 95% by volume of pores, and/or the

electrode active material loading is no less than 20 mg/cm². The conductive porous layer thickness is most preferably from 400 μ m to 5 mm.

In certain embodiments, the conductive porous layer structure is selected from metal foam, metal web or screen, perforated metal sheet-based 3-D structure, metal fiber mat, metal nanowire mat, conductive polymer nano-fiber mat, conductive polymer foam, conductive polymer-coated fiber foam, carbon foam, graphite foam, carbon aerogel, carbon xerox gel, graphene foam, graphene oxide foam, reduced graphene oxide foam, carbon fiber foam, graphite fiber foam, exfoliated graphite foam, or a combination thereof.

As a supercapacitor active material, graphene sheets may be selected from the group consisting of pristine graphene, graphene oxide, reduced graphene oxide, graphene fluoride, graphene chloride, graphene bromide, graphene iodide, hydrogenated graphene, nitrogenated graphene, boron-doped graphene, nitrogen-doped graphene, chemically functionalized graphene, physically or chemically activated or etched versions thereof, and combinations thereof. In an embodiment, the anode or the cathode contains graphene sheets as the only electrode active material and does not contain any other electrode active material.

In certain embodiments, the anode or the cathode contains the following materials as the only electrode active material in the anode or cathode: (a) graphene sheets alone; (b) graphene sheets mixed with a carbon material; (c) graphene sheets mixed with a partner material that forms a redox pair with the graphene sheets to develop pseudo-capacitance; or (d) graphene sheets and a carbon material mixed with a partner material (e.g. a conducting polymer or metal oxide) that forms a redox pair with graphene sheets or the carbon material to develop pseudo-capacitance, and wherein there is no other electrode active material in the anode or cathode.

The anode active material and the cathode active material can be the same material or different materials. Preferably, the volume ratio of the anode active material-to-liquid electrolyte in the first dispersion is from 1/5 to 20/1 (preferably from 1/3 to 5/1) and/or the volume ratio of cathode active material-to-the liquid electrolyte in the second dispersion is from 1/5 to 20/1 (preferably from 1/3 to 5/1).

In certain embodiments, the anode active material or cathode active material contains a carbon and/or graphene material and further contains a redox pair partner material selected from a metal oxide, a conducting polymer, an organic material, a non-graphene carbon material, an inorganic material, or a combination thereof, wherein the partner material, in combination with graphene or a carbon material, form a redox pair for developing pseudo-capacitance. The metal oxide may be selected from RuO₂, IrO₂, NiO, MnO₂, VO₂, V₂O₅, V₃O₈, TiO₂, Cr₂O₃, Co₂O₃, Co₃O₄, PbO₂, Ag₂O, or a combination thereof. The inorganic material may be selected from a metal carbide, metal nitride, metal boride, metal dichalcogenide, or a combination thereof. Conducting polymers preferably contain an intrinsically conductive polymer, such as polyacetylene, polypyrrole, polyaniline, polythiophene, or their derivatives.

In some embodiments, the metal oxide or inorganic material may be selected from an oxide, dichalcogenide, trichalcogenide, sulfide, selenide, or telluride of niobium, zirconium, molybdenum, hafnium, tantalum, tungsten, titanium, vanadium, chromium, cobalt, manganese, iron, or nickel in a nanowire, nano-disc, nano-ribbon, or nano platelet form. Preferably, the inorganic material is selected from nano discs, nano platelets, nano-coating, or nano sheets of an inorganic material selected from: (a) bismuth selenide or bismuth telluride, (b) transition metal dichalcogenide or trichalcogenide, (c) sulfide, selenide, or telluride of niobium, zirconium, molybdenum, hafnium, tantalum, tungsten, titanium, cobalt, manganese, iron, nickel, or a transition metal; (d) boron nitride, or (e) a combination thereof; wherein the discs, platelets, or sheets have a thickness less than 100 nm.

In an embodiment, we have a supercapacitor-type cathode (an electric double layer or redox pair type electrode), but the anode is a battery-like anode that intercalates/de-intercalates lithium or sodium ions (e.g. containing pre-lithiated graphite particles, pre-sodiated carbon particles, or pre-lithiated Si particles) and the resulting supercapacitor is a lithium ion capacitor or sodium-ion capacitor (still a capacitor, not a battery). Thus, the invention also provides a process for producing a special class of supercapacitor cell (i.e. a lithium ion capacitor, LIC, or sodium-ion capacitor, NIC).

Such a process includes: (A) preparing a plurality of electrically conductive porous layers and a plurality of wet cathode layers each composed of a cathode active material (e.g. activated

carbon particles and/or graphene sheets) and an optional conductive additive mixed with a liquid or gel electrolyte, wherein the conductive porous layers contain interconnected conductive pathways and at least 80% by volume of pores; and (B) stacking and consolidating a desired number of the porous layers and a desired number of the wet cathode layers in an alternating sequence to form a cathode electrode having a thickness no less than 100 μm .; (C) supplying an anode electrode, which contains a pre-lithiated or pre-sodiated anode active material; and (D) stacking the anode electrode, a porous separator, and the cathode electrode to form a lithium-ion capacitor or sodium-ion capacitor, wherein the cathode electrode has a thickness no less than 100 μm (preferably > 200 μm , more preferably > 300 μm , further more preferably > 400 μm , still more preferably > 500 μm , and most preferably > 600 μm) and the cathode active material constitutes an electrode active material loading no less than 7 mg/cm^2 in said cathode electrode. Preferably, the cathode active material constitutes an electrode active material loading no less than 10 mg/cm^2 (preferably > 20 mg/cm^2 , more preferably > 30 mg/cm^2 , still more preferably > 50 mg/cm^2 , and most preferably > 100 mg/cm^2).

There are at least two ways to prepare the anode electrode layer; the conventional process and the presently invented process. The conventional process includes mixing graphite particles in NMP solvent to form a slurry, which is coated on one or two surfaces of an anode current collector (e.g. non-porous, thin Cu foil). The solvent is then removed to obtain dried electrode and a liquid electrolyte is injected into the anode side after the battery cell is assembled and housed in a packaging envelop. More preferably, the anode electrode for the presently invented LIC or NIC is also made by the presently invented process described above. This inventive process includes (A) Continuously feeding a second electrically conductive porous layer to an anode material impregnation zone, wherein the second conductive porous layer has two opposed porous surfaces and contain interconnected electron-conducting pathways and, preferably, at least 70% by volume of pores; and (B) Impregnating a wet anode active material mixture into the second electrically conductive porous layer from at least one of the two porous surfaces to form an electrode. The wet anode active material mixture contains a liquid electrolyte and an anode active material selected from prelithiated or pre-sodiated versions of graphite particles, carbon

particles, Si nano particles, Sn nano particles, or any other commonly used anode active materials for lithium-ion batteries or sodium-ion batteries.

In a lithium-ion capacitor (LIC), the anode active material may be selected from the group consisting of: (a) Pre-lithiated particles of natural graphite, artificial graphite, meso-carbon microbeads (MCMB), and carbon; (b) Pre-lithiated particles or coating of Silicon (Si), germanium (Ge), tin (Sn), lead (Pb), antimony (Sb), bismuth (Bi), zinc (Zn), aluminum (Al), nickel (Ni), cobalt (Co), manganese (Mn), titanium (Ti), iron (Fe), and cadmium (Cd); (c) Pre-lithiated alloys or intermetallic compounds of Si, Ge, Sn, Pb, Sb, Bi, Zn, Al, or Cd with other elements, wherein said alloys or compounds are stoichiometric or non-stoichiometric; (d) Pre-lithiated oxides, carbides, nitrides, sulfides, phosphides, selenides, and tellurides of Si, Ge, Sn, Pb, Sb, Bi, Zn, Al, Fe, Ni, Co, Ti, Mn, or Cd, and their mixtures or composites; and (e) Pre-lithiated graphene sheets; and combinations thereof.

In a sodium-ion capacitor, the anode active material contains a pre-sodiated version of petroleum coke, carbon black, amorphous carbon, activated carbon, hard carbon, soft carbon, templated carbon, hollow carbon nanowires, hollow carbon sphere, or titanate, or a sodium intercalation compound selected from $\text{NaTi}_2(\text{PO}_4)_3$, $\text{Na}_2\text{Ti}_3\text{O}_7$, $\text{Na}_2\text{C}_8\text{H}_4\text{O}_4$, Na_2TP , Na_xTiO_2 ($x = 0.2$ to 1.0), $\text{Na}_2\text{C}_8\text{H}_4\text{O}_4$, carboxylate based material, $\text{C}_8\text{H}_4\text{Na}_2\text{O}_4$, $\text{C}_8\text{H}_6\text{O}_4$, $\text{C}_8\text{H}_5\text{NaO}_4$, $\text{C}_8\text{Na}_2\text{F}_4\text{O}_4$, $\text{C}_{10}\text{H}_2\text{Na}_4\text{O}_8$, $\text{C}_{14}\text{H}_4\text{O}_6$, $\text{C}_{14}\text{H}_4\text{Na}_4\text{O}_8$, or a combination thereof.

In a sodium-ion capacitor, the anode active material contains a sodium intercalation compound selected from the following groups of materials: (a) Sodium-doped silicon (Si), germanium (Ge), tin (Sn), lead (Pb), antimony (Sb), bismuth (Bi), zinc (Zn), aluminum (Al), titanium (Ti), cobalt (Co), nickel (Ni), manganese (Mn), cadmium (Cd), and mixtures thereof; (b) Sodium-containing alloys or intermetallic compounds of Si, Ge, Sn, Pb, Sb, Bi, Zn, Al, Ti, Co, Ni, Mn, Cd, and their mixtures; (c) Sodium-containing oxides, carbides, nitrides, sulfides, phosphides, selenides, tellurides, or antimonides of Si, Ge, Sn, Pb, Sb, Bi, Zn, Al, Fe, Ti, Co, Ni, Mn, Cd, and mixtures or composites thereof; (d) Sodium salts; and (e) Graphene sheets pre-loaded with sodium or potassium.

BRIEF DESCRIPTION OF THE DRAWINGS

FIG.1(A) Schematic of a prior art supercapacitor cell.

FIG.1(B) Schematic of a presently invented supercapacitor cell, comprising an anode electrode 251 composed of a conductive porous layer (e.g. an anode current collector in the form of a highly porous foam or several porous foam sheets stacked together) impregnated with a wet anode active material mixture (e.g. liquid electrolyte and an anode active material and optional conductive additive), a porous separator, and a cathode electrode 253 composed of a current collector in the form of a highly porous foam (or several foam sheets stacked together) impregnated with a wet cathode active material mixture.

FIG.1(C) Schematic of a presently invented supercapacitor cell comprising (i) a stack of alternately placed conductive porous layers and wet anode layers, (ii) a porous separator, and (iii) a stack of alternately configured conductive porous layers and wet cathode layers prior to consolidation (e.g. via compression) of multiple porous layers (as a backbone of a current collector) and wet electrode layers together to achieve infiltration of porous layers by the anode active material and liquid electrolyte (and optional conductive additive) to form the anode electrode and prior to infiltration of porous layers by the cathode active material and liquid electrolyte (and optional conductive additive) to form the cathode electrode.

FIG.1(D) Schematic of a presently invented supercapacitor cell, as illustrated in Fig. 1(C), but after consolidation (e.g. via compression) of multiple porous layers (as a backbone of a current collector) and wet electrode layers together to achieve infiltration of porous layers by the anode active material and liquid electrolyte (and optional conductive additive) to form the anode electrode and after infiltration of porous layers by the cathode active material and liquid electrolyte (and optional conductive additive) to form the cathode electrode.

FIG.1(E) Schematic of a presently invented process for producing a supercapacitor cell (a lithium-ion or sodium-ion capacitor) by combining and laminating an anode electrode, separator, and cathode electrode; the cathode electrode is prepared by a presently invented process of compressing alternately stacked conductive porous layers and wet cathode layers.

FIG.2 An electron microscopic image of typical graphene sheets.

FIG.3(A) Examples of conductive porous layers: metal grid/mesh and carbon nano-fiber mat.

FIG.3(B) Examples of conductive porous layers: graphene foam and carbon foam.

FIG.3(C) Examples of conductive porous layers: graphite foam and Ni foam.

FIG.3(D) Examples of conductive porous layers: Cu foam and stainless steel foam.

FIG.4(A) Schematic of a commonly used process for producing exfoliated graphite, expanded graphite flakes (thickness > 100 nm), and graphene sheets (thickness < 100 nm, more typically < 10 nm, and can be as thin as 0.34 nm)

FIG.4 (B) Schematic drawing to illustrate the processes for producing exfoliated graphite, expanded graphite flakes, and graphene sheets.

FIG.5 Ragone plots (gravimetric and volumetric power density vs. energy density) of symmetric supercapacitor (EDLC) cells containing reduced graphene oxide (RGO) sheets as the electrode active material and EMIMBF4 ionic liquid electrolyte. Supercapacitors were prepared according to an embodiment of instant invention and, for comparison, by the conventional slurry coating of electrodes.

FIG.6 Ragone plots (gravimetric and volumetric power density vs. energy density) of symmetric supercapacitor (EDLC) cells containing activated carbon (AC) particles as the electrode active material and organic liquid electrolyte. Supercapacitors were prepared according to an embodiment of instant invention and by the conventional slurry coating of electrodes.

FIG.7(A) Ragone plots (gravimetric and volumetric power density vs. energy density) of lithium ion capacitor (LIC) cells containing pristine graphene sheets as the electrode active material and lithium salt-PC/DEC organic liquid electrolyte. Supercapacitors were prepared according to an embodiment of instant invention and by the conventional slurry coating of electrodes.

FIG.7(B) Ragone plots (gravimetric and volumetric power density vs. energy density) of sodium ion capacitor (NIC) cells containing pristine graphene sheets as the electrode active material and sodium salt-PC/DEC organic liquid electrolyte.

FIG.8 The cell-level gravimetric and volumetric energy densities plotted over the achievable electrode thickness range of the AC-based EDLC supercapacitors prepared via the conventional method and the presently invented method. Legends: the gravimetric (♦)

and volumetric (\blacktriangle) energy density of the conventional supercapacitors and the gravimetric (\blacksquare) and volumetric (\times) energy density of the inventive supercapacitors. With the presently invented method, there is no theoretical limit on the electrode thickness that can be achieved. Typically, the practical electrode thickness is from 10 μm to 1000 μm , more typically from 100 μm to 800 μm , and most typically from 200 μm to 600 μm .

FIG.9 The cell-level gravimetric and volumetric energy densities plotted over the achievable electrode thickness range of the RGO-based EDLC supercapacitors (organic liquid electrolyte) prepared via the conventional method and the presently invented method. Legends: the gravimetric (\blacklozenge) and volumetric (\blacktriangle) energy density of the conventional supercapacitors (highest achieved electrode tap density of approximately 0.25 g/cm^3) and the gravimetric (\blacksquare) and volumetric (\times) energy density of the inventive supercapacitors (easily achieved electrode tap density of approximately 0.75 g/cm^3).

FIG.10 The cell-level gravimetric and volumetric energy densities plotted over the achievable electrode thickness range of the pristine graphene-based EDLC supercapacitors (organic liquid electrolyte) prepared via the conventional method and the presently invented method. Legends: the gravimetric (\blacklozenge) and volumetric (\blacktriangle) energy density of the conventional supercapacitors (highest achieved electrode tap density of approximately 0.25 g/cm^3) and the gravimetric (\blacksquare) and volumetric (\times) energy density of the inventive supercapacitors (electrode tap density of approximately 1.15 g/cm^3).

FIG.11 The cell-level gravimetric and volumetric energy densities plotted over the achievable electrode thickness range of the pristine graphene-based EDLC supercapacitors (ionic liquid electrolyte) prepared via the conventional method and the presently invented method. Legends: the gravimetric (\blacklozenge) and volumetric (\blacktriangle) energy density of the conventional supercapacitors (highest achieved electrode tap density of approximately 0.25 g/cm^3) and the gravimetric (\blacksquare) and volumetric (\times) energy density of the inventive supercapacitors (electrode tap density of approximately 1.15 g/cm^3).

FIG.12 The cell-level gravimetric energy densities plotted over the achievable active material proportion (active material weight/total cell weight) for activated carbon-based EDLC supercapacitors (with organic liquid electrolyte).

FIG.13 The cell-level gravimetric energy densities plotted over the achievable active material proportion (active material weight/total cell weight) in a supercapacitor cell for two series of pristine graphene-based EDLC supercapacitors (all with organic liquid electrolyte).

FIG.14 The cell-level volumetric energy densities plotted over the achievable active material proportion (active material weight/total cell weight) for pristine graphene-based EDLC supercapacitors (with ionic liquid electrolyte).

DESCRIPTION OF THE PREFERRED EMBODIMENTS

The present invention may be understood more readily by reference to the following detailed description of the invention taken in connection with the accompanying drawing figures, which form a part of this disclosure. It is to be understood that this invention is not limited to the specific devices, methods, conditions or parameters described and/or shown herein, and that the terminology used herein is for the purpose of describing particular embodiments by way of example only and is not intended to be limiting of the claimed invention.

As schematically illustrated in FIG. 1(A), a prior art supercapacitor cell is typically composed of an anode current collector 202 (e.g. Al foil 12-15 μm thick), an anode active material layer 204 (containing an anode active material, such as activated carbon particles 232 and conductive additives that are bonded by a resin binder, such as PVDF), a porous separator 230, a cathode active material layer 208 (containing a cathode active material, such as activated carbon particles 234, and conductive additives that are all bonded by a resin binder, not shown), a cathode current collector 206 (e.g. Al foil), and a liquid electrolyte disposed in both the anode active material layer 204 (also simply referred to as the “anode layer”) and the cathode active material layer 208 (or simply “cathode layer”). The entire cell is encased in a protective housing, such as a thin plastic-aluminum foil laminate-based envelop. The prior art supercapacitor cell is typically made by a process that includes the following steps:

- a) The first step is mixing particles of the anode active material (e.g. activated carbon), a conductive filler (e.g. graphite flakes), a resin binder (e.g. PVDF) in a solvent (e.g. NMP) to form an anode slurry. On a separate basis, particles of the cathode active material (e.g. activated carbon), a conductive filler (e.g. acetylene black), a resin binder (e.g. PVDF) are mixed and dispersed in a solvent (e.g. NMP) to form a cathode slurry.

- b) The second step includes coating the anode slurry onto one or both primary surfaces of an anode current collector (e.g. Cu or Al foil), drying the coated layer by vaporizing the solvent (e.g. NMP) to form a dried anode electrode coated on Cu or Al foil. Similarly, the cathode slurry is coated and dried to form a dried cathode electrode coated on Al foil.
- c) The third step includes laminating an anode/Al foil sheet, a porous separator layer, and a cathode/Al foil sheet together to form a 3-layer or 5-layer assembly, which is cut and slit into desired sizes and stacked to form a rectangular structure (as an example of shape) or rolled into a cylindrical cell structure.
- d) The rectangular or cylindrical laminated structure is then encased in an aluminum-plastic laminated envelope or steel casing.
- e) A liquid electrolyte is then injected into the laminated structure to make a supercapacitor cell.

There are several serious problems associated with this conventional process and the resulting supercapacitor cell:

- 1) It is very difficult to produce an activated carbon-based electrode layer (anode layer or cathode layer) that is thicker than 100 μm and practically impossible or impractical to produce an electrode layer thicker than 200 μm . There are several reasons why this is the case:
 - a. An electrode of 100 μm thickness typically requires a heating zone of 30-50 meters long in a slurry coating facility, which is too time consuming, too energy intensive, and not cost-effective.
 - b. Thicker electrodes have a great tendency to get delaminated and cracked.
 - c. For some electrode active materials, such as graphene sheets, it has not been possible to produce an electrode thicker than 50 μm in a real manufacturing environment on a continuous basis. This is despite the notion that some thicker electrodes have been claimed in open or patent literature; these electrodes were prepared in a laboratory on a small scale. In a laboratory setting, presumably one could repeatedly add new materials to a layer and manually consolidate the layer to increase the thickness of an

electrode. However, even with such a manual procedure (not amenable to mass production), the resulting electrode becomes very fragile and brittle.

- d. This problem is even worse for graphene-based electrodes, since repeated compressions lead to re-stacking of graphene sheets and, hence, significantly reduced specific surface area and reduced specific capacitance.
- 2) With a conventional process, as depicted in FIG. 1(A), the actual mass loadings of the electrodes and the apparent densities for the active materials are too low. In most cases, the active material mass loadings of the electrodes (areal density) is significantly lower than 10 mg/cm² and the apparent volume density or tap density of the active material is typically less than 0.75 g/cm³ (more typically less than 0.5 g/cm³ and most typically less than 0.3 g/cm³) even for relatively large particles of activated carbon. In addition, there are other non-active materials (e.g. conductive additive and resin binder) that add additional weights and volumes to the electrode without contributing to the cell capacity. These low areal densities and low volume densities result in relatively low volumetric capacitances and low volumetric energy density.
- 3) The conventional process requires dispersing electrode active materials (anode active material and cathode active material) in a liquid solvent (e.g. NMP) to make a slurry and, upon coating on a current collector surface, the liquid solvent has to be removed to dry the electrode layer. Once the anode and cathode layers, along with a separator layer, are laminated together and packaged in a housing to make a supercapacitor cell, one then injects a liquid electrolyte into the cell. In actuality, one makes the two electrodes wet, then makes the electrodes dry, and finally makes them wet again. Such a wet-dry-wet process does not sound like a good process at all.
- 4) Current supercapacitors (e.g. symmetric supercapacitors or electric double layer capacitors, EDLC) still suffer from a relatively low gravimetric energy density and low volumetric energy density. Commercially available EDLCs exhibit a gravimetric energy density of approximately 6 Wh/kg and no experimental EDLC cells have been reported to exhibit an energy density higher than 10 Wh/kg (based on the total cell weight) at room temperature. Although experimental supercapacitors exhibit large volumetric electrode capacitances (100 to 200 F/cm³ in most cases) at the electrode level (not the cell level),

the typical active mass loading of <1 mg/cm², tap density of < 0.1 g/cm³, and electrode thicknesses of up to tens of micrometers of these experimental cells remain significantly lower than those used in most commercially available electrochemical capacitors, resulting in energy storage devices with relatively low areal and volumetric capacities and low volumetric energy densities based on the cell (device) weight.

In literature, the energy density data reported based on either the active material weight alone or electrode weight cannot directly translate into the energy densities of a practical supercapacitor cell or device. The “overhead weight” or weights of other device components (binder, conductive additive, current collectors, separator, electrolyte, and packaging) must also be taken into account. The convention production process results in an active material proportion being less than 30% by weight of the total cell weight ($< 15\%$ in some cases; e.g. for graphene-based active material).

The present invention provides a method of producing a supercapacitor cell having a high electrode thickness (thickness of the electrode that contains electrode active materials), high active material mass loading, low overhead weight and volume, high volumetric capacitance, and high volumetric energy density. In addition, the manufacturing costs of the supercapacitors produced by the presently invented process are significantly lower than those by conventional processes.

As illustrated in FIG. 1(B), the presently invented supercapacitor cell comprises a conductive porous layer (e.g. an anode current collector in the form of a highly porous foam) impregnated with a wet anode active material mixture (e.g. liquid electrolyte and an anode active material and an optional conductive additive), a porous separator, and another conductive porous layer (e.g. a cathode current collector in the form of a highly porous foam) impregnated with a wet cathode active material mixture. The pores (e.g. 250a) in the anode side are filled with an anode active material (e.g. graphene sheets, 252a) and liquid electrolyte (254a), plus optional modifying additives.

The present invention provides a process for producing a supercapacitor cell having a large electrode thickness, high active material mass loading, low overhead weight and volume

(relative to active materials), high volumetric capacitance, and high volumetric energy density.

In one embodiment, as illustrated in FIG. 1(C) and 1(D), the invented process comprises:

- (A) Preparing a plurality of electrically conductive porous layers (e.g. 240a, 240b at the anode side and 242a, 242b at the cathode side), a plurality of wet anode layers (e.g. 236a, 236b) of an anode active material and an optional conductive additive mixed with a first liquid electrolyte, and a plurality of wet cathode layers (e.g. 238a, 238b) of a cathode active material and an optional conductive additive mixed with a second liquid electrolyte, wherein the conductive porous layers contain interconnected electron-conducting pathways and at least 70% (preferably at least 80%) by volume of pores;
- (B) Stacking and consolidating a desired number of porous layers and a desired number of wet anode layers in a preferably alternating sequence (e.g. 244, shown prior to consolidation) to form an anode electrode (e.g. 264 in Fig. 1(D), after consolidation) having a thickness no less than 100 μm (preferably $> 200 \mu\text{m}$, further preferably $> 300 \mu\text{m}$, more preferably $> 400 \mu\text{m}$; further more preferably $> 500 \mu\text{m}$, $600 \mu\text{m}$, or even $> 1,000 \mu\text{m}$; no theoretical limitation on this anode thickness). Consolidation may involve the application of a compressive stress to force the wet anode layer ingredients to infiltrate into the pores of the multiple conductive porous layers. These multiple conductive porous layers are also compressed together to form an anode current collector that essentially extends over the thickness of the entire anode electrode 264;
- (C) Placing a porous separator layer (241 in Fig. 3(C) or 3(D)) in contact with the anode electrode;
- (D) Stacking and consolidating a desired number of conductive porous layers and a desired number of wet cathode layers preferably in an alternating sequence (e.g. 246, shown prior to consolidation) to form a cathode electrode (e.g. 262 in Fig. 1(D), after consolidation) in contact with the porous separator 241, wherein the cathode electrode has a thickness no less than 100 μm ; wherein step (D) is conducted before or after step (B); The cathode thickness is preferably $> 200 \mu\text{m}$, further preferably $> 300 \mu\text{m}$, more preferably $> 400 \mu\text{m}$; further more preferably $> 500 \mu\text{m}$, $600 \mu\text{m}$, or even $> 1,000 \mu\text{m}$; no theoretical limitation on this cathode thickness. Consolidation may involve the application of a compressive stress to force the wet cathode layer ingredients to infiltrate into the pores of

the multiple conductive porous layers. These multiple conductive porous layers are also compressed together to form a cathode current collector that essentially extends over the entire thickness of the cathode electrode **262**; and

(E) Assembling and sealing the anode electrode, porous separator, and cathode electrode in a housing to produce the lithium battery;

In this battery, the anode active material or cathode active material has a material mass loading no less than 7 mg/cm^2 (preferably and typically higher than 10 mg/cm^2 , more preferably and typically no less than 20 mg/cm^2 , and even more preferably and typically higher than 30 mg/cm^2).

For illustration purposes, if we pick a small zone **250** in the anode **264**, we will find anode active material particles **252** (plus optional conductive additive) dispersed in a liquid electrolyte. Also, both the active material and the liquid electrolyte are lodged in pores of the current collector (conductive porous layer that substantially extends over the entire anode electrode). If we pick a small zone **260** in the cathode, we will find cathode material particles (plus optional conductive additive) dispersed in a liquid electrolyte, and both the cathode active material and the liquid electrolyte reside in pores of the current collector (also extending over substantially the entire cathode electrode thickness).

The electrically conductive porous layers may be selected from metal foam, metal web or screen, perforated metal sheet-based structure, metal fiber mat, metal nanowire mat, conductive polymer nano-fiber mat, conductive polymer foam, conductive polymer-coated fiber foam, carbon foam, graphite foam, carbon aerogel, carbon xerox gel, graphene foam, graphene oxide foam, reduced graphene oxide foam, carbon fiber foam, graphite fiber foam, exfoliated graphite foam, or a combination thereof. The porous layers must be made of an electrically conductive material, such as a carbon, graphite, metal, metal-coated fiber, and conductive polymer, which is in a form of highly porous mat, screen/grid, non-woven, foam, etc. Examples of conductive porous layers are presented in Fig. 3(A), 3(B), 3(C), and 3(D). The porosity level must be at least 70% by volume, preferably greater than 80%, further preferably greater than 90%, and most preferably greater than 95% by volume. The backbone or foam walls form a network of electron-conducting pathways.

Preferably, substantially all of the pores in the original conductive porous layers are filled with the electrode (anode or cathode) active material, optional conductive additive, and liquid electrolyte (no binder resin needed). Since there are great amounts of pores (80-99%) relative to the pore walls or conductive pathways (1-20%), very little space is wasted (“being wasted” means not being occupied by the electrode active material and electrolyte), resulting in high amounts of electrode active material-electrolyte zones (high active material loading mass).

An alternative configuration, schematically illustrated in FIG.1(E), is a presently invented lithium-ion capacitor cell, comprising an anode current collector 280 containing a layer of anode active material (e.g. pre-lithiated graphite particles) 282 deposited thereon, a porous separator 284, and a stack 288 of alternatingly arranged conductive porous layers (e.g. 274a, 274b), intended for use as a constituent of a cathode current collector, and wet cathode layers (e.g. 272a, 272b) prior to being consolidated (compressed). Upon consolidation, the cathode active material and the liquid electrolyte (along with any optional conductive additive) are forced to permeate into pores of the conductive porous layers, which are also compressed to form a cathode layer 290. As shown here, the pores 270 of this foamed current collector have been impregnated with a mixture of cathode active material particles and liquid electrolyte.

In such configurations (FIG. 1(C)-(E)), the electrons only have to travel a short distance (half of the pore size, on average; e.g. a few micrometers) before they are collected by the current collector (pore walls) since pore walls are present everywhere throughout the entire current collector (also the entire anode layer). Additionally, in each wet anode layer or wet cathode layer, all electrode active material particles are pre-dispersed in a liquid electrolyte (no wettability issue), eliminating the existence of dry pockets commonly present in an electrode prepared by the conventional process of wet coating, drying, packing, and electrolyte injection. Thus, the presently invented process produces a totally unexpected advantage over the conventional supercapacitor cell production process.

The above are but several examples to illustrate how the presently invented supercapacitor electrodes and supercapacitor cells can be made continuously, in an automated manner. These examples should not be construed as limiting the scope of the instant invention.

The first and/or second conductive porous layer has a thickness no less than 100 μm (preferably greater than 200 μm , more preferably greater than 300 μm , further preferably greater than 400 μm , and most preferably greater than 500 μm ; no theoretical limit on the electrode thickness) and preferably at least 80% by volume of pores (preferably at least 85% porosity, more preferably at least 90%, and most preferably at least 95%). These porous layer structures have essentially a porosity level of 80%-99% and remaining 1%-20% being pore walls (e.g. metal or graphite skeleton). These pores are used to accommodate a mixture of active materials (e.g. graphene sheets) and liquid electrolyte, where electric double layers of charges or redox pairs are present when the supercapacitor is charged.

Preferably, substantially all of the pores in the porous layer are filled with the electrode (anode or cathode) active material and liquid electrolyte. The anode active material may be the same as or different from the cathode active material. Since there are great amounts of pores (80-99%) relative to the pore walls (1-20%), very little space is wasted (“being wasted” means not being occupied by the electrode active material and electrolyte), resulting in high amounts of electrode active material-electrolyte zones (high active material loading mass).

Schematically shown in FIG. 1(B) is an embodiment of the presently invented supercapacitor cell having large electrode thicknesses and large length; there is no limitation on the thickness or length of the cell. Both the electrically conductive porous layer in the anode (e.g. anode current collector foam) and the conductive porous layer at the cathode (e.g. cathode current collector foam) have been impregnated with their respective wet electrode active material mixtures. As an example, a pore 250, in an enlarged view, is filled with the wet anode active material mixture containing graphene sheets 252 (an example of an electrode active material) and liquid electrolyte layers 254 that are closely packed in an alternating manner. Such a tight packing enables us to achieve a high tap density (packing density) of the active material that otherwise cannot be achieved by any existing process.

In such a configuration, the charges (electrons) only have to travel a short distance (half of the pore size, on average; e.g. a few micrometers) before they are collected by the current collector (pore walls). Additionally, in each wet electrode active material mixture, graphene sheets are dispersed in a liquid electrolyte (i.e. each graphene sheet is surrounded by liquid

electrolyte). Upon impregnation into the pores of the porous layers (as the anode or cathode current collector), the slurry (wet mixture) remains in a dispersion or suspension state, in which individual graphene sheets remain surrounded by the liquid electrolyte, totally eliminating the possibility of graphene sheets being fully re-stacked that otherwise would result in the specific surface area being significantly reduced. Thus, the presently invented process produces a totally unexpected advantage over the conventional supercapacitor cell production process.

In a preferred embodiment, the graphene electrode material is selected from pristine graphene, graphene oxide, reduced graphene oxide, graphene fluoride, graphene chloride, graphene bromide, graphene iodide, hydrogenated graphene, nitrogenated graphene, chemically functionalized graphene, or a combination thereof. The starting graphitic material for producing any one of the above graphene materials may be selected from natural graphite, artificial graphite, meso-phase carbon, meso-phase pitch, meso-carbon micro-bead, soft carbon, hard carbon, coke, carbon fiber, carbon nano-fiber, carbon nano-tube, or a combination thereof.

The present invention also provides a lithium-ion capacitor (LIC) or a sodium-ion capacitor (NIC), wherein at least one of the two electrodes is produced by the presently invented process. More preferably, both the anode electrode and the cathode electrode for the presently invented LIC or NIC are made by the presently invented process described above.

This inventive process includes (A) Preparing a plurality of electrically conductive porous layers and a plurality of wet electrode layers composed of an electrode active material (i.e. a cathode active material) and an optional conductive additive mixed with a liquid or gel electrolyte, wherein the conductive porous layers contain interconnected conductive pathways and at least 80% by volume of pores; (B) Stacking and consolidating a desired number of the porous layers and a desired number of the wet electrode layers to form an electrode having a thickness no less than 100 μm ; (C) supplying an anode electrode, which contains a pre-lithiated or pre-sodiated anode active material; and (D) stacking the anode electrode, a porous separator, and the cathode electrode to form a lithium-ion capacitor or sodium-ion capacitor.

In an embodiment, the cathode active material contains multiple particles of a carbon material and/or multiple graphene sheets, wherein multiple graphene sheets contain single-layer

graphene or few-layer graphene each having from 1 to 10 graphene planes and said multiple particles of carbon material have a specific surface area no less than 500 m²/g when measured in a dried state.

The anode electrode may also be prepared by using the presently invented sequential stacking of porous conductive layers with wet anode electrode layers, followed by consolidation. The wet anode active material mixture lodged in pores of a conductive porous layer preferably contains a liquid electrolyte and an anode active material preferably selected from prelithiated or pre-sodiated versions of graphite particles, carbon particles, Si nano particles, Sn nano particles, or any other commonly used anode active materials for lithium-ion batteries or sodium-ion batteries. These anode active materials can be made into a fine particle form and multiple particles, along with conductive additive particles, can be readily mixed with a liquid electrolyte to form a wet anode active material mixture layer for stacking with a conductive porous layer.

In a lithium-ion capacitor (LIC), the anode active material may be selected from the group consisting of: (a) Pre-lithiated particles of natural graphite, artificial graphite, meso-carbon microbeads (MCMB), and carbon; (b) Pre-lithiated particles or coating of Silicon (Si), germanium (Ge), tin (Sn), lead (Pb), antimony (Sb), bismuth (Bi), zinc (Zn), aluminum (Al), nickel (Ni), cobalt (Co), manganese (Mn), titanium (Ti), iron (Fe), and cadmium (Cd); (c) Pre-lithiated alloys or intermetallic compounds of Si, Ge, Sn, Pb, Sb, Bi, Zn, Al, or Cd with other elements, wherein said alloys or compounds are stoichiometric or non-stoichiometric; (d) Pre-lithiated oxides, carbides, nitrides, sulfides, phosphides, selenides, and tellurides of Si, Ge, Sn, Pb, Sb, Bi, Zn, Al, Fe, Ni, Co, Ti, Mn, or Cd, and their mixtures or composites; and (e) Pre-lithiated graphene sheets; and combinations thereof. Pre-lithiation can be accomplished electrochemically by using a compact mass of graphene sheets as the working electrode and lithium metal as the counter electrode. Pre-lithiation may also be accomplished by adding lithium powder or chips along with the anode active material (e.g. Si particles) and conductive additive particles into a liquid electrolyte.

In a preferred sodium-ion capacitor, the anode active material contains a pre-sodiated version of petroleum coke, carbon black, amorphous carbon, activated carbon, hard carbon, soft carbon, templated carbon, hollow carbon nanowires, hollow carbon sphere, or titanate, or a

sodium intercalation compound selected from $\text{NaTi}_2(\text{PO}_4)_3$, $\text{Na}_2\text{Ti}_3\text{O}_7$, $\text{Na}_2\text{C}_8\text{H}_4\text{O}_4$, Na_2TP , Na_xTiO_2 ($x = 0.2$ to 1.0), $\text{Na}_2\text{C}_8\text{H}_4\text{O}_4$, carboxylate based material, $\text{C}_8\text{H}_4\text{Na}_2\text{O}_4$, $\text{C}_8\text{H}_6\text{O}_4$, $\text{C}_8\text{H}_5\text{NaO}_4$, $\text{C}_8\text{Na}_2\text{F}_4\text{O}_4$, $\text{C}_{10}\text{H}_2\text{Na}_4\text{O}_8$, $\text{C}_{14}\text{H}_4\text{O}_6$, $\text{C}_{14}\text{H}_4\text{Na}_4\text{O}_8$, or a combination thereof.

Bulk natural graphite is a 3-D graphitic material with each graphite particle being composed of multiple grains (a grain being a graphite single crystal or crystallite) with grain boundaries (amorphous or defect zones) demarcating neighboring graphite single crystals. Each grain is composed of multiple graphene planes that are oriented parallel to one another. A graphene plane in a graphite crystallite is composed of carbon atoms occupying a two-dimensional, hexagonal lattice. In a given grain or single crystal, the graphene planes are stacked and bonded via van der Waal forces in the crystallographic *c*-direction (perpendicular to the graphene plane or basal plane). Although all the graphene planes in one grain are parallel to one another, typically the graphene planes in one grain and the graphene planes in an adjacent grain are inclined at different orientations. In other words, the orientations of the various grains in a graphite particle typically differ from one grain to another.

The constituent graphene planes of a graphite crystallite in a natural or artificial graphite particle can be exfoliated and extracted or isolated to obtain individual graphene sheets of hexagonal carbon atoms, which are single-atom thick, provided the inter-planar van der Waals forces can be overcome. An isolated, individual graphene plane of carbon atoms is commonly referred to as single-layer graphene. A stack of multiple graphene planes bonded through van der Waals forces in the thickness direction with an inter-graphene plane spacing of approximately 0.3354 nm is commonly referred to as a multi-layer graphene. A multi-layer graphene platelet has up to 300 layers of graphene planes (< 100 nm in thickness), but more typically up to 30 graphene planes (< 10 nm in thickness), even more typically up to 20 graphene planes (< 7 nm in thickness), and most typically up to 10 graphene planes (commonly referred to as few-layer graphene in scientific community). Single-layer graphene and multi-layer graphene sheets are collectively called “nano graphene platelets” (NGPs). Graphene sheets/platelets (collectively, NGPs) are a new class of carbon nano material (a 2-D nano carbon) that is distinct from the 0-D fullerene, the 1-D CNT or CNF, and the 3-D graphite. For the purpose of defining the claims and

as is commonly understood in the art, a graphene material (isolated graphene sheets) is not (and does not include) a carbon nanotube (CNT) or a carbon nano-fiber (CNF).

Our research group pioneered the development of graphene materials and related production processes as early as 2002: (1) B. Z. Jang and W. C. Huang, “Nano-scaled Graphene Plates,” U.S. Pat. No. 7,071,258 (07/04/2006), application submitted on October 21, 2002; (2) B. Z. Jang, et al. “Process for Producing Nano-scaled Graphene Plates,” U.S. Patent Application No. 10/858,814 (06/03/2004); and (3) B. Z. Jang, A. Zhamu, and J. Guo, “Process for Producing Nano-scaled Platelets and Nanocomposites,” US Pat. Application No. 11/509,424 (08/25/2006).

In one process, graphene materials are obtained by intercalating natural graphite particles with a strong acid and/or an oxidizing agent to obtain a graphite intercalation compound (GIC) or graphite oxide (GO), as illustrated in FIG. 4(A) and FIG. 4(B) (schematic drawings). The presence of chemical species or functional groups in the interstitial spaces between graphene planes in a GIC or GO serves to increase the inter-graphene spacing (d_{002} , as determined by X-ray diffraction), thereby significantly reducing the van der Waals forces that otherwise hold graphene planes together along the c -axis direction. The GIC or GO is most often produced by immersing natural graphite powder (100 in FIG. 4(B)) in a mixture of sulfuric acid, nitric acid (an oxidizing agent), and another oxidizing agent (e.g. potassium permanganate or sodium perchlorate). The resulting GIC (102) is actually some type of graphite oxide (GO) particles if an oxidizing agent is present during the intercalation procedure. This GIC or GO is then repeatedly washed and rinsed in water to remove excess acids, resulting in a graphite oxide suspension or dispersion, which contains discrete and visually discernible graphite oxide particles dispersed in water. In order to produce graphene materials, one can follow one of the two processing routes after this rinsing step, briefly described below:

Route 1 involves removing water from the suspension to obtain “expandable graphite,” which is essentially a mass of dried GIC or dried graphite oxide particles. Upon exposure of expandable graphite to a temperature in the range of typically 800 – 1,050°C for approximately 30 seconds to 2 minutes, the GIC undergoes a rapid volume expansion by a factor of 30-300 to form “graphite worms” (104), which are each a collection of exfoliated, but largely un-separated graphite flakes that remain interconnected.

In Route 1A, these graphite worms (exfoliated graphite or “networks of interconnected/non-separated graphite flakes”) can be re-compressed to obtain flexible graphite sheets or foils (106) that typically have a thickness in the range of 0.1 mm (100 μm) - 0.5 mm (500 μm). Alternatively, one may choose to use a low-intensity air mill or shearing machine to simply break up the graphite worms for the purpose of producing the so-called “expanded graphite flakes” (108) which contain mostly graphite flakes or platelets thicker than 100 nm (hence, not a nano material by definition).

In Route 1B, the exfoliated graphite is subjected to high-intensity mechanical shearing (e.g. using an ultrasonicator, high-shear mixer, high-intensity air jet mill, or high-energy ball mill) to form separated single-layer and multi-layer graphene sheets (collectively called NGPs, 112), as disclosed in our US Application No. 10/858,814 (06/03/2004). Single-layer graphene can be as thin as 0.34 nm, while multi-layer graphene can have a thickness up to 100 nm, but more typically less than 10 nm (commonly referred to as few-layer graphene). Multiple graphene sheets or platelets may be made into a sheet of NGP paper using a paper-making process. This sheet of NGP paper is an example of the porous graphene structure layer utilized in the presently invented process.

Route 2 entails ultrasonication of the graphite oxide suspension (e.g. graphite oxide particles dispersed in water) for the purpose of separating/isolating individual graphene oxide sheets from graphite oxide particles. This is based on the notion that the inter-graphene plane separation has been increased from 0.3354 nm in natural graphite to 0.6-1.1 nm in highly oxidized graphite oxide, significantly weakening the van der Waals forces that hold neighboring planes together. Ultrasonic power can be sufficient to further separate graphene plane sheets to form fully separated, isolated, or discrete graphene oxide (GO) sheets. These graphene oxide sheets can then be chemically or thermally reduced to obtain “reduced graphene oxides” (RGO) typically having an oxygen content of 0.001%-10% by weight, more typically 0.01%-5% by weight, most typically and preferably less than 2% by weight of oxygen.

For the purpose of defining the claims of the instant application, NGPs or graphene materials include discrete sheets/platelets of single-layer and multi-layer (typically less than 10 layers) pristine graphene, graphene oxide, reduced graphene oxide (RGO), graphene fluoride,

graphene chloride, graphene bromide, graphene iodide, hydrogenated graphene, nitrogenated graphene, chemically functionalized graphene, doped graphene (e.g. doped by B or N). Pristine graphene has essentially 0% oxygen. RGO typically has an oxygen content of 0.001%-5% by weight. Graphene oxide (including RGO) can have 0.001%-50% by weight of oxygen. Other than pristine graphene, all the graphene materials have 0.001%-50% by weight of non-carbon elements (e.g. O, H, N, B, F, Cl, Br, I, etc.). These materials are herein referred to as non-pristine graphene materials.

Pristine graphene, in smaller discrete graphene sheets (typically 0.3 μm to 10 μm), may be produced by direct ultrasonication (also known as liquid phase exfoliation or production) or supercritical fluid exfoliation of graphite particles. These processes are well-known in the art.

The graphene oxide (GO) may be obtained by immersing powders or filaments of a starting graphitic material (e.g. natural graphite powder) in an oxidizing liquid medium (e.g. a mixture of sulfuric acid, nitric acid, and potassium permanganate) in a reaction vessel at a desired temperature for a period of time (typically from 0.5 to 96 hours, depending upon the nature of the starting material and the type of oxidizing agent used). As previously described above, the resulting graphite oxide particles may then be subjected to thermal exfoliation or ultrasonic wave-induced exfoliation to produce isolated GO sheets. These GO sheets can then be converted into various graphene materials by substituting –OH groups with other chemical groups (e.g. –Br, NH_2 , etc.).

Fluorinated graphene or graphene fluoride is herein used as an example of the halogenated graphene material group. There are two different approaches that have been followed to produce fluorinated graphene: (1) fluorination of pre-synthesized graphene: This approach entails treating graphene prepared by mechanical exfoliation or by CVD growth with fluorinating agent such as XeF_2 , or F-based plasmas; (2) Exfoliation of multilayered graphite fluorides: Both mechanical exfoliation and liquid phase exfoliation of graphite fluoride can be readily accomplished.

Interaction of F_2 with graphite at high temperature leads to covalent graphite fluorides $(\text{CF})_n$ or $(\text{C}_2\text{F})_n$, while at low temperatures graphite intercalation compounds (GIC) C_xF ($2 \leq x \leq$

24) form. In $(CF)_n$ carbon atoms are sp^3 -hybridized and thus the fluorocarbon layers are corrugated consisting of trans-linked cyclohexane chairs. In $(C_2F)_n$ only half of the C atoms are fluorinated and every pair of the adjacent carbon sheets are linked together by covalent C–C bonds. Systematic studies on the fluorination reaction showed that the resulting F/C ratio is largely dependent on the fluorination temperature, the partial pressure of the fluorine in the fluorinating gas, and physical characteristics of the graphite precursor, including the degree of graphitization, particle size, and specific surface area. In addition to fluorine (F_2), other fluorinating agents may be used, although most of the available literature involves fluorination with F_2 gas, sometimes in presence of fluorides.

For exfoliating a layered precursor material to the state of individual layers or few-layers, it is necessary to overcome the attractive forces between adjacent layers and to further stabilize the layers. This may be achieved by either covalent modification of the graphene surface by functional groups or by non-covalent modification using specific solvents, surfactants, polymers, or donor-acceptor aromatic molecules. The process of liquid phase exfoliation includes ultrasonic treatment of a graphite fluoride in a liquid medium.

The nitrogenation of graphene can be conducted by exposing a graphene material, such as graphene oxide, to ammonia at high temperatures (200–400°C). Nitrogenated graphene could also be formed at lower temperatures by a hydrothermal method; e.g. by sealing GO and ammonia in an autoclave and then increased the temperature to 150–250°C. Other methods to synthesize nitrogen doped graphene include nitrogen plasma treatment on graphene, arc-discharge between graphite electrodes in the presence of ammonia, ammonolysis of graphene oxide under CVD conditions, and hydrothermal treatment of graphene oxide and urea at different temperatures.

The aforementioned features are further described and explained in detail as follows: As illustrated in FIG. 4(B), a graphite particle (e.g. 100) is typically composed of multiple graphite crystallites or grains. A graphite crystallite is made up of layer planes of hexagonal networks of carbon atoms. These layer planes of hexagonally arranged carbon atoms are substantially flat and are oriented or ordered so as to be substantially parallel and equidistant to one another in a particular crystallite. These layers of hexagonal-structured carbon atoms, commonly referred to

as graphene layers or basal planes, are weakly bonded together in their thickness direction (crystallographic *c*-axis direction) by weak van der Waals forces and groups of these graphene layers are arranged in crystallites. The graphite crystallite structure is usually characterized in terms of two axes or directions: the *c*-axis direction and the *a*-axis (or *b*-axis) direction. The *c*-axis is the direction perpendicular to the basal planes. The *a*- or *b*-axes are the directions parallel to the basal planes (perpendicular to the *c*-axis direction).

A highly ordered graphite particle can consist of crystallites of a considerable size, having a length of L_a along the crystallographic *a*-axis direction, a width of L_b along the crystallographic *b*-axis direction, and a thickness L_c along the crystallographic *c*-axis direction. The constituent graphene planes of a crystallite are highly aligned or oriented with respect to each other and, hence, these anisotropic structures give rise to many properties that are highly directional. For instance, the thermal and electrical conductivity of a crystallite are of great magnitude along the plane directions (*a*- or *b*-axis directions), but relatively low in the perpendicular direction (*c*-axis). As illustrated in the upper-left portion of FIG. 4(B), different crystallites in a graphite particle are typically oriented in different directions and, hence, a particular property of a multi-crystallite graphite particle is the directional average value of all the constituent crystallites.

Due to the weak van der Waals forces holding the parallel graphene layers, natural graphite can be treated so that the spacing between the graphene layers can be appreciably opened up so as to provide a marked expansion in the *c*-axis direction, and thus form an expanded graphite structure in which the laminar character of the carbon layers is substantially retained. The process for manufacturing flexible graphite is well-known in the art. In general, flakes of natural graphite (e.g. 100 in FIG. 4(B)) are intercalated in an acid solution to produce graphite intercalation compounds (GICs, 102). The GICs are washed, dried, and then exfoliated by exposure to a high temperature for a short period of time. This causes the flakes to expand or exfoliate in the *c*-axis direction of the graphite up to 80-300 times of their original dimensions. The exfoliated graphite flakes are vermiform in appearance and, hence, are commonly referred to as graphite worms 104. These worms of graphite flakes which have been greatly expanded can be formed without the use of a binder into cohesive or integrated sheets of expanded graphite,

e.g. webs, papers, strips, tapes, foils, mats or the like (typically referred to as "flexible graphite" 106) having a typical density of about 0.04-2.0 g/cm³ for most applications.

Acids, such as sulfuric acid, are not the only type of intercalating agent (intercalant) that penetrate into spaces between graphene planes to obtain GICs. Many other types of intercalating agents, such as alkali metals (Li, K, Na, Cs, and their alloys or eutectics), can be used to intercalate graphite to stage 1, stage 2, stage 3, etc. Stage *n* implies one intercalant layer for every *n* graphene planes. For instance, a stage-1 potassium-intercalated GIC means there is one layer of K for every graphene plane; or, one can find one layer of K atoms inserted between two adjacent graphene planes in a G/K/G/K/G/KG sequence, where G is a graphene plane and K is a potassium atom plane. A stage-2 GIC will have a sequence of GG/K/GG/K/GG/K/GG and a stage-3 GIC will have a sequence of GGG/K/GGG/K/GGG, etc. These GICs can then be brought in contact with water or water-alcohol mixture to produce exfoliated graphite and/or separated/isolated graphene sheets.

Exfoliated graphite worms may be subjected to high-intensity mechanical shearing/separation treatments using a high-intensity air jet mill, high-intensity ball mill, or ultrasonic device to produce separated nano graphene platelets (NGPs) with all the graphene platelets thinner than 100 nm, mostly thinner than 10 nm, and, in many cases, being single-layer graphene (also illustrated as 112 in FIG. 4(B)). An NGP is composed of a graphene sheet or a plurality of graphene sheets with each sheet being a two-dimensional, hexagonal structure of carbon atoms. A mass of multiple NGPs (including discrete sheets/platelets of single-layer and/or few-layer graphene or graphene oxide may be made into a graphene film/paper (114 in FIG. 4(B)) using a film- or paper-making process. Alternatively, with a low-intensity shearing, graphite worms tend to be separated into the so-called expanded graphite flakes (108 in FIG. 4(B) having a thickness > 100 nm. These flakes can be formed into graphite paper or mat 106 using a paper- or mat-making process, with or without a resin binder.

Despite the fact that individual graphene sheets have an exceptionally high specific surface area, graphene sheets have a great tendency to re-stack together or to overlap with one another, thereby dramatically reducing the specific capacitance due to the significantly reduced specific surface area that is accessible by the electrolyte. This tendency to re-stack is particularly

acute during the supercapacitor cell electrode production process. In this process, graphene sheets, along with other conductive additive and resin binder (e.g. PVDF), are dispersed in a solvent (typically NMP) to form a slurry, which is then coated on a surface of a solid current collector (e.g. Al foil). The solvent is then removed (vaporized) to form a dried layer of active material electrode, which is then fed through a pair of rollers in a compression machine to consolidate the electrode layer. These drying and compressing procedures induce severe graphene re-stacking. In many of the scientific reports, even though the graphene sheets in an original powder form were found to exhibit an exceptionally high specific surface area, the resulting electrode only shows an unexpectedly lower specific capacitance. Theoretically, the maximum specific capacitance of a single-layer graphene-based supercapacitor is as high as 550 F/g (based on an EDLC structure, no redox pair or pseudo-capacitance), but experimentally achieved values have been in the range of mere 90-170 F/g. This has been a long-standing problem in the art of supercapacitors.

The present invention provides a highly innovative and elegant process to overcome this graphene sheet re-stacking issue. This invented process completely eliminates the need to go through slurry coating, drying, and compressing procedures. Instead of forming a slurry containing an environmentally undesirable solvent (i.e. NMP), the process entails dispersing graphene sheets in a liquid electrolyte to form a wet layer of electrode active material-liquid electrolyte mixture. Multiple wet mixture layers are then stacked with multiple conductive porous layers in an alternating sequence and the resulting stack is then compressed to enable consolidation (active material-electrolyte impregnated into pores of a conductive foam-based current collector). No subsequent solvent removal and electrolyte injection are required, and no or little possibility of graphene sheets being re-stacked together. Furthermore, graphene sheets are already pre-dispersed in a liquid electrolyte, implying that essentially all graphene surfaces are naturally accessible to the electrolyte, leaving behind no “dry pockets”. This process also enables us to pack graphene sheets (with electrolyte in between) in a highly compact manner, giving rise to an unexpectedly high electrode active material tap density.

The graphene sheets used in the aforementioned process may be subjected to the following treatments, separately or in combination, prior to being mixed with a liquid or gel electrolyte:

- (a) Being chemically functionalized or doped with atomic, ionic, or molecular species. Useful surface functional groups may include quinone, hydroquinone, quaternized aromatic amines, mercaptans, or disulfides. This class of functional groups can impart pseudo-capacitance to graphene-based supercapacitors.
- (b) Coated or grafted with an intrinsically conductive polymer (conducting polymers, such as polyacetylene, polypyrrole, polyaniline, polythiophene, and their derivatives, are good choices for use in the present invention); These treatments are intended for further increasing the capacitance value through pseudo-capacitance effects such as redox reactions.
- (c) Deposition with transition metal oxides or sulfides, such as RuO₂, TiO₂, MnO₂, Cr₂O₃, and Co₂O₃, for the purpose of forming redox pairs with graphene sheets, thereby imparting pseudo-capacitance to the electrode; and
- (d) Subjected to an activation treatment (analogous to activation of carbon black materials) to create additional surfaces and possibly imparting functional chemical groups to these surfaces. The activation treatment can be accomplished through CO₂ physical activation, KOH chemical activation, or exposure to nitric acid, fluorine, or ammonia plasma.

We have discovered that a wide variety of two-dimensional (2D) inorganic materials can be used in the presented invented supercapacitors prepared by the invented active material-electrolyte impregnation process. Layered materials represent a diverse source of 2D systems that can exhibit unexpected electronic properties and high specific surface areas that are important for Supercapacitor applications. Although graphite is the best known layered material, transition metal dichalcogenides (TMDs), transition metal oxides (TMOs), and a broad array of other compounds, such as BN, Bi₂Te₃, and Bi₂Se₃, are also potential sources of 2D materials.

Non-graphene 2D nano materials, single-layer or few-layer (up to 20 layers), can be produced by several methods: mechanical cleavage, laser ablation (e.g. using laser pulses to ablate TMDs down to a single layer), liquid phase exfoliation, and synthesis by thin film

techniques, such as PVD (e.g. sputtering), evaporation, vapor phase epitaxy, liquid phase epitaxy, chemical vapor epitaxy, molecular beam epitaxy (MBE), atomic layer epitaxy (ALE), and their plasma-assisted versions.

We have surprisingly discovered that most of these inorganic materials, when in a 2D nano-disc, nano-platelet, nano-belt, or nano-ribbon form, exhibit remarkable EDLC values, even though these inorganic materials are normally considered as electrically non-conducting and, hence, not a candidate supercapacitor electrode material. The supercapacitance values are exceptionally high when these 2D nano materials are used in combination with a small amount of nano graphene sheets (particularly single-layer graphene). The required single-layer graphene can be from 0.1% to 50% by weight, more preferably from 0.5% to 25%, and most preferably from 1% to 15% by weight.

In the instant invention, there is no limitation on the type of liquid electrolytes that can be used in the supercapacitor: aqueous, organic, gel, and ionic liquid. Typically, electrolytes for supercapacitors consist of solvent and dissolved chemicals (e.g. salts) that dissociate into positive ions (cations) and negative ions (anions), making the electrolyte electrically conductive. The more ions the electrolyte contains, the better its conductivity, which also influences the capacitance. In supercapacitors, the electrolyte provides the molecules for the separating monolayer in the Helmholtz double-layer (electric double layer) and delivers the ions for pseudocapacitance.

Water is a relatively good solvent for dissolving inorganic chemicals. When added together with acids such as sulfuric acid (H_2SO_4), alkalis such as potassium hydroxide (KOH), or salts such as quaternary phosphonium salts, sodium perchlorate ($NaClO_4$), lithium perchlorate ($LiClO_4$) or lithium hexafluoride arsenate ($LiAsF_6$), water offers relatively high conductivity values. Aqueous electrolytes have a dissociation voltage of 1.15 V per electrode and a relatively low operating temperature range. Water electrolyte-based supercapacitors exhibit low energy density.

Alternatively, electrolytes may contain organic solvents, such as acetonitrile, propylene carbonate, tetrahydrofuran, diethyl carbonate, γ -butyrolactone, and solutes with quaternary

ammonium salts or alkyl ammonium salts such as tetraethylammonium tetrafluoroborate ($\text{N}(\text{Et})_4\text{BF}_4$) or triethyl (methyl) tetrafluoroborate ($\text{NMe}(\text{Et})_3\text{BF}_4$). Organic electrolytes are more expensive than aqueous electrolytes, but they have a higher dissociation voltage of typically 1.35 V per electrode (2.7 V capacitor voltage), and a higher temperature range. The lower electrical conductivity of organic solvents (10 to 60 mS/cm) leads to a lower power density, but a higher energy density since the energy density is proportional to the square of the voltage.

The ionic liquid is composed of ions only. Ionic liquids are low melting temperature salts that are in a molten or liquid state when above a desired temperature. For instance, a salt is considered as an ionic liquid if its melting point is below 100°C. If the melting temperature is equal to or lower than room temperature (25°C), the salt is referred to as a room temperature ionic liquid (RTIL). The IL salts are characterized by weak interactions, due to the combination of a large cation and a charge-delocalized anion. This results in a low tendency to crystallize due to flexibility (anion) and asymmetry (cation).

A typical and well-known ionic liquid is formed by the combination of a 1-ethyl-3-methylimidazolium (EMI) cation and an *N,N*-bis(trifluoromethane)sulphonamide (TFSI) anion. This combination gives a fluid with an ionic conductivity comparable to many organic electrolyte solutions and a low decomposition propensity and low vapor pressure up to ~300-400°C. This implies a generally low volatility and non-flammability and, hence, a much safer electrolyte for batteries.

Ionic liquids are basically composed of organic ions that come in an essentially unlimited number of structural variations owing to the preparation ease of a large variety of their components. Thus, various kinds of salts can be used to design the ionic liquid that has the desired properties for a given application. These include, among others, imidazolium, pyrrolidinium and quaternary ammonium salts as cations and bis(trifluoromethanesulphonyl) imide, bis(fluorosulphonyl)imide, and hexafluorophosphate as anions. Based on their compositions, ionic liquids come in different classes that basically include aprotic, protic and zwitterionic types, each one suitable for a specific application.

Common cations of room temperature ionic liquids (RTILs) include, but not limited to, tetraalkylammonium, di-, tri-, and tetra-alkylimidazolium, alkylpyridinium, dialkyl-pyrrolidinium, dialkylpiperidinium, tetraalkylphosphonium, and trialkylsulfonium. Common anions of RTILs include, but not limited to, BF_4^- , $\text{B}(\text{CN})_4^-$, CH_3BF_3^- , $\text{CH}_2\text{CHBF}_3^-$, CF_3BF_3^- , $\text{C}_2\text{F}_5\text{BF}_3^-$, $n\text{-C}_3\text{F}_7\text{BF}_3^-$, $n\text{-C}_4\text{F}_9\text{BF}_3^-$, PF_6^- , CF_3CO_2^- , CF_3SO_3^- , $\text{N}(\text{SO}_2\text{CF}_3)_2^-$, $\text{N}(\text{COCF}_3)(\text{SO}_2\text{CF}_3)^-$, $\text{N}(\text{SO}_2\text{F})_2^-$, $\text{N}(\text{CN})_2^-$, $\text{C}(\text{CN})_3^-$, SCN^- , SeCN^- , CuCl_2^- , AlCl_4^- , $\text{F}(\text{HF})_{2.3}^-$, etc. Relatively speaking, the combination of imidazolium- or sulfonium-based cations and complex halide anions such as AlCl_4^- , BF_4^- , CF_3CO_2^- , CF_3SO_3^- , NTf_2^- , $\text{N}(\text{SO}_2\text{F})_2^-$, or $\text{F}(\text{HF})_{2.3}^-$ results in RTILs with good working conductivities.

RTILs can possess archetypical properties such as high intrinsic ionic conductivity, high thermal stability, low volatility, low (practically zero) vapor pressure, non-flammability, the ability to remain liquid at a wide range of temperatures above and below room temperature, high polarity, high viscosity, and wide electrochemical windows. These properties, except for the high viscosity, are desirable attributes when it comes to using an RTIL as an electrolyte ingredient (a salt and/or a solvent) in a supercapacitor.

In order to make a pseudo-capacitor (a supercapacitor that works on the development of pseudo-capacitance through redox pair formation), the anode active material or cathode active material may be designed to contain graphene sheets and a redox pair partner material selected from a metal oxide, a conducting polymer, an organic material, a non-graphene carbon material, an inorganic material, or a combination thereof. Many of the materials that can pair up with reduced graphene oxide sheets are well-known in the art. In this study, we have come to realize that graphene halogenide (e.g. graphene fluoride), graphene hydrogenide, and nitrogenated graphene can work with a wide variety of partner materials to form a redox pair for developing pseudo-capacitance.

For instance, the metal oxide or inorganic materials that serve in such a role include RuO_2 , IrO_2 , NiO , MnO_2 , VO_2 , V_2O_5 , V_3O_8 , TiO_2 , Cr_2O_3 , Co_2O_3 , Co_3O_4 , PbO_2 , Ag_2O , MoC_x , Mo_2N , or a combination thereof. In general, the inorganic material may be selected from a metal carbide, metal nitride, metal boride, metal dichalcogenide, or a combination thereof. Preferably, the desired metal oxide or inorganic material is selected from an oxide, dichalcogenide,

trichalcogenide, sulfide, selenide, or telluride of niobium, zirconium, molybdenum, hafnium, tantalum, tungsten, titanium, vanadium, chromium, cobalt, manganese, iron, or nickel in a nanowire, nano-disc, nano-ribbon, or nano platelet form. These materials can be in the form of a simple mixture with sheets of a graphene material, but preferably in a nano particle or nano coating form that is physically or chemically bonded to a surface of the graphene sheets prior to being formed into a wet active material mixture (e.g. in a slurry form) and impregnated into the pores of the conductive porous layers.

In what follows, we provide some examples of several different types of graphene materials, other types of electrode active materials (e.g. activated carbon and select inorganic materials), redox pair partner materials, and porous current collector materials (e.g. graphite foam, graphene foam, and metal foam) to illustrate the best mode of practicing the instant invention. These illustrative examples and other portions of instant specification and drawings, separately or in combinations, are more than adequate to enable a person of ordinary skill in the art to practice the instant invention. However, these examples should not be construed as limiting the scope of instant invention.

EXAMPLE 1: Supercapacitors containing reduced graphene oxide (RGO) sheets

Single-layer reduced graphene oxide sheets were obtained from Angstrom Materials, Inc., Dayton, Ohio. Two separate processes were conducted to prepare supercapacitor cells featuring RGO and RGO-carbon mixtures as electrode active materials. One process was conducted according to the presently invented alternating stacking of active material-electrolyte mixture layers and foamed current collector layers (conductive porous layers). For comparison, the other process was the conventional one that included the steps of slurry coating on solid current collectors (Al foil, 12 μm thick), removal of NMP solvent to produce dried electrode layers coated on current collectors, lamination of coated current collectors and a separator disposed between the two current collectors, encasing of the laminated structure, and injection of liquid electrolyte into the encased cell.

In one series of samples, activated carbon (AC) particles and multi-walled carbon nanotubes (CNT) were separately added into the RGO-electrolyte suspensions, with an AC-to-GO ratio of 5/95 and CNT-to-RGO ratio of 10/90, respectively, to prepare the active material-

electrolyte layers. Typically, 1-6 layers of Ni foam (each layer 200 μm thick, having a 95% porosity level as the conductive porous layers) were stacked together with the active material-electrolyte mixture layers, resulting in an electrode layer of approximately 200-1,200 μm thick. Supercapacitor cells containing pure RGO sheets alone as the electrode active material were also made and tested.

In the present study, electrode active materials were also chosen based on graphene sheets in combination with an inorganic material, which included nano discs, nano platelets, or nano sheets of an inorganic material selected from: (a) bismuth selenide, (b) transition metal dichalcogenide: sulfide or selenide of zirconium, molybdenum, titanium, cobalt, manganese, iron, and nickel; and (c) boron nitride.

EXAMPLE 2: Preparation of graphene oxide (GO) and reduced graphene oxide (RGO) nano sheets from natural graphite powder

Natural graphite from Huadong Graphite Co. (Qingdao, China) was used as the starting material. GO was obtained by following the well-known modified Hummers method, which involved two oxidation stages. In a typical procedure, the first oxidation was achieved in the following conditions: 1,100 mg of graphite was placed in a 1,000 mL boiling flask. Then, 20 g of $\text{K}_2\text{S}_2\text{O}_8$, 20 g of P_2O_5 , and 400 mL of a concentrated aqueous solution of H_2SO_4 (96%) were added in the flask. The mixture was heated under reflux for 6 hours and then let without disturbing for 20 hours at room temperature. Oxidized graphite was filtered and rinsed with abundant distilled water until neutral pH. A wet cake-like material was recovered at the end of this first oxidation.

For the second oxidation process, the previously collected wet cake was placed in a boiling flask that contains 69 mL of a concentrated aqueous solution of H_2SO_4 (96%). The flask was kept in an ice bath as 9 g of KMnO_4 was slowly added. Care was taken to avoid overheating. The resulting mixture was stirred at 35°C for 2 hours (the sample color turning dark green), followed by the addition of 140 mL of water. After 15 min, the reaction was halted by adding 420 mL of water and 15 mL of an aqueous solution of 30 wt % H_2O_2 . The color of the sample at this stage turned bright yellow. To remove the metallic ions, the mixture was filtered and rinsed with a 1:10 HCl aqueous solution. The collected material was gently centrifuged at 2700g and

rinsed with deionized water. The final product was a wet cake that contained 1.4 wt % of GO, as estimated from dry extracts. Subsequently, liquid dispersions of GO platelets were obtained by lightly sonicating wet-cake materials, which were diluted in deionized water.

Surfactant-stabilized RGO (RGO-BS) was obtained by diluting the wet-cake in an aqueous solution of surfactants instead of pure water. A commercially available mixture of cholate sodium (50 wt. %) and deoxycholate sodium (50 wt. %) salts provided by Sigma Aldrich was used. The surfactant weight fraction was 0.5 wt. %. This fraction remains the same for all samples. Sonication was performed using a Branson Sonifier S-250A equipped with a 13 mm step disruptor horn and a 3 mm tapered micro-tip, operating at a 20 kHz frequency. For instance, 10 mL of aqueous solutions containing 0.1 wt. % of GO was sonicated for 10 min and subsequently centrifuged at 2700g for 30 min to remove any non-dissolved large particles, aggregates, and impurities. Chemical reduction of as-obtained GO to yield RGO was conducted by following the method, which involved placing 10 mL of a 0.1 wt. % GO aqueous solution in a boiling flask of 50 mL. Then, 10 μ L of a 35 wt. % aqueous solution of N_2H_4 (hydrazine) and 70 mL of a 28 wt. % of an aqueous solution of NH_4OH (ammonia) were added to the mixture, which was stabilized by surfactants. The solution was heated to 90°C and refluxed for 1 h. The pH value measured after the reaction was approximately 9. The color of the sample turned dark black during the reduction reaction.

After chemical reduction of GO to become RGO, the dried RGO powder was dispersed in an organic electrolyte (acetonitrile + $\text{N}(\text{Et})_4\text{BF}_4$) to form viscous (gel-like) layers of organic electrolyte-RGO mixture. GO powder was separately mixed with sulfuric acid-based electrolyte mixture to form aqueous electrolyte-GO gel. The gel-like layers were then separately stacked sequentially with two separate sets of conductive porous layers (Ni foam) to produce two separate EDLC supercapacitor cells.

For comparison purposes, conventional slurry coating and drying procedures were conducted to produce conventional electrodes. Electrodes and a separator disposed between two electrodes were then assembled and encased in an Al-plastic laminated packaging envelop, followed by liquid electrolyte injection to form a supercapacitor cell.

Example 3: Preparation of single-layer graphene sheets from meso-carbon micro-beads (MCMBs)

Meso-carbon microbeads (MCMBs) were supplied from China Steel Chemical Co., Kaohsiung, Taiwan. This material has a density of about 2.24 g/cm^3 with a median particle size of about $16 \mu\text{m}$. MCMB (10 grams) were intercalated with an acid solution (sulfuric acid, nitric acid, and potassium permanganate at a ratio of 4:1:0.05) for 48-96 hours. Upon completion of the reaction, the mixture was poured into deionized water and filtered. The intercalated MCMBs were repeatedly washed in a 5% solution of HCl to remove most of the sulphate ions. The sample was then washed repeatedly with deionized water until the pH of the filtrate was no less than 4.5. The slurry was then subjected ultrasonication for 10-100 minutes to produce GO suspensions. TEM and atomic force microscopic studies indicate that most of the GO sheets were single-layer graphene when the oxidation treatment exceeded 72 hours, and 2- or 3-layer graphene when the oxidation time was from 48 to 72 hours.

The GO sheets contain oxygen proportion of approximately 35%-47% by weight for oxidation treatment times of 48-96 hours. GO sheets were suspended in water and then dried to produce GP powder. The GO powder was then thermally reduced at 200-700°C for varying periods of time to produce samples of reduced graphene oxide (RGO) powder having an oxygen content of approximately from 1% to 20%. These RGOs were used directly as an EDLC-type supercapacitor electrode active material or join a partner material (e.g. metal oxide, NiO_2 , or conducting polymer, polypyrrole, bonded to RGO surface) to form a redox pair in a pseudo-capacitance based supercapacitor. Both the presently invented process and conventional process were used to produce supercapacitor cells, which were electrochemically tested and compared.

Example 4: Preparation of pristine graphene sheets (0% oxygen) as a supercapacitor electrode active material

Recognizing the possibility of the high defect population in GO sheets acting to reduce the conductivity of individual graphene plane, we decided to study if the use of pristine graphene sheets (non-oxidized and oxygen-free, non-halogenated and halogen-free, etc.) can lead to a graphene foam having a higher thermal conductivity. Pristine graphene sheets were produced by using the well-known direct ultrasonication or liquid-phase exfoliation process.

In a typical procedure, five grams of graphite flakes, ground to approximately 20 μm or less in sizes, were dispersed in 1,000 mL of deionized water (containing 0.1% by weight of a dispersing agent, Zonyl® FSO from DuPont) to obtain a suspension. An ultrasonic energy level of 85 W (Branson S450 Ultrasonicator) was used for exfoliation, separation, and size reduction of graphene sheets for a period of 15 minutes to 2 hours. The resulting graphene sheets are pristine graphene that have never been oxidized and are oxygen-free and relatively defect-free. Pristine graphene is essentially free from any non-carbon elements. Pristine graphene sheets were then incorporated in a supercapacitor using both the presently invented procedure of active material-electrolyte layers and conductive porous layers being alternately stacked and consolidated, and conventional procedure of slurry coating, drying and layer laminating. Both EDLC and pseudo-capacitance types (redox pair with polyaniline or MnO_2) of supercapacitors were investigated.

Example 5: CVD graphene foam-based current collectors (conductive porous layers) prepared on Ni foam templates

The procedure for producing CVD graphene foam was adapted from that disclosed in open literature: Chen, Z. et al. "Three-dimensional flexible and conductive interconnected graphene networks grown by chemical vapor deposition," *Nature Materials*, 10, 424–428 (2011). Nickel foam, a porous structure with an interconnected 3D scaffold of nickel was chosen as a template for the growth of graphene foam. Briefly, carbon was introduced into a nickel foam by decomposing CH_4 at 1,000°C under ambient pressure, and graphene films were then deposited on the surface of the nickel foam. Due to the difference in the thermal expansion coefficients between nickel and graphene, ripples and wrinkles were formed on the graphene films. Four types of foams made in this example were used as a current collector in the presently invented supercapacitors: Ni foam, CVD graphene-coated Ni form, CVD graphene foam (Ni being etched away), and conductive polymer bonded CVD graphene foam.

In order to recover (separate) graphene foam from the Ni template, Ni template was etched away. In the procedure proposed by Chen, et al., before etching away the nickel skeleton by a hot HCl (or FeCl_3) solution, a thin layer of poly(methyl methacrylate) (PMMA) was deposited on the surface of the graphene films as a support to prevent the graphene network from

collapsing during nickel etching. After the PMMA layer was carefully removed by hot acetone, a fragile graphene foam sample was obtained. The use of the PMMA support layer was considered critical to preparing a free-standing film of graphene foam. Instead, we used a conducting polymer as a binder resin to hold graphene together while Ni was etched away. It may be noted that the CVD graphene foam used herein is intended as a foamed current collector to accommodate the carbon particles or graphene sheets along with a liquid electrolyte. But, we have surprisingly found that such a graphene foam, with or without a conductive polymer, is itself a supercapacitor electrode material. Such a combination enables a maximized amount of active materials incorporated in a supercapacitor cell.

Example 6: Graphitic foam-based current collectors from pitch-based carbon foams

Pitch powder, granules, or pellets were placed in an aluminum mold with the desired final shape of the foam. Mitsubishi ARA-24 meso-phase pitch was utilized. The sample was evacuated to less than 1 torr and then heated to a temperature approximately 300°C. At this point, the vacuum was released to a nitrogen blanket and then a pressure of up to 1,000 psi was applied. The temperature of the system was then raised to 800°C. This was performed at a rate of 2 degrees C/min. The temperature was held constant for at least 15 minutes and then the furnace power was turned off and cooled to room temperature at a rate of approximately 1.5 degrees C/min with a pressure release rate of approximately 2 psi/min. Final foam temperatures were 630°C and 800°C. During the cooling cycle, pressure is released gradually to atmospheric conditions. The foam was then heat treated to 1050°C (carbonized) under a nitrogen blanket and then heat treated in separate runs in a graphite crucible to 2500°C and 2800°C (graphitized) in Argon.

Example 7: Preparation of graphene fluoride sheets as a supercapacitor active material

Several processes have been used by us to produce GF, but only one process is herein described as an example. In a typical procedure, highly exfoliated graphite (HEG) was prepared from intercalated compound $C_2F \cdot xClF_3$. HEG was further fluorinated by vapors of chlorine trifluoride to yield fluorinated highly exfoliated graphite (FHEG). Pre-cooled Teflon reactor was filled with 20–30 mL of liquid pre-cooled ClF_3 , the reactor was closed and cooled to liquid nitrogen temperature. Then, no more than 1 g of HEG was put in a container with holes for ClF_3

gas to access and situated inside the reactor. In 7–10 days a gray-beige product with approximate formula C₂F was formed.

Subsequently, a small amount of FHEG (approximately 0.5 mg) was mixed with 20–30 mL of an organic solvent (methanol and ethanol, separately) and subjected to an ultrasound treatment (280 W) for 30 min, leading to the formation of homogeneous yellowish dispersions. Upon removal of solvent, the dispersion became a brownish powder.

Example 8: Preparation of nitrogenataed graphene sheets as a supercapacitor electrode active material

Graphene oxide (GO), synthesized in Example 2, was finely ground with different proportions of urea and the pelletized mixture heated in a microwave reactor (900 W) for 30 s. The product was washed several times with deionized water and vacuum dried. In this method graphene oxide gets simultaneously reduced and doped with nitrogen. The products obtained with graphene : urea mass ratios of 1 : 0.5, 1 : 1 and 1 : 2 are designated as NGO-1, NGO-2 and NGO-3 respectively and the nitrogen contents of these samples were 14.7, 18.2 and 17.5 wt% respectively as found by elemental analysis. These nitrogenataed graphene sheets remain dispersible in water. The resulting suspensions were then dried to obtain nitrogenated graphene powder. The powder was mixed with an ionic liquid electrolyte to form gel-like layers for impregnation into pores of conductive porous layers in a sequential stacking operation.

EXAMPLE 9: Preparation of MoS₂/RGO hybrid material as a supercapacitor active material

A wide variety of inorganic materials were investigated in this example. For instance, an ultra-thin MoS₂/RGO hybrid was synthesized by a one-step solvothermal reaction of (NH₄)₂MoS₄ and hydrazine in an *N, N*-dimethylformamide (DMF) solution of oxidized graphene oxide (GO) at 200°C. In a typical procedure, 22 mg of (NH₄)₂MoS₄ was added to 10 mg of GO dispersed in 10 ml of DMF. The mixture was sonicated at room temperature for approximately 10 min until a clear and homogeneous solution was obtained. After that, 0.1 ml of N₂H₄•H₂O was added. The reaction solution was further sonicated for 30 min before being transferred to a 40 mL Teflon-lined autoclave. The system was heated in an oven at 200°C for 10 h. Product was collected by centrifugation at 8000 rpm for 5 min, washed with DI water and recollected by centrifugation. The washing step was repeated 5 times to ensure that most DMF was removed.

Finally, product was dried and mixed with liquid electrolyte to form active material-electrolyte mixture layers, which were stacked alternately with Al foam layers and consolidated. On a separate basis, several different amounts (5% to 45% by weight) of MoS₂ platelets were combined with activated carbon particles to form a composite electrode active material. This composite active material was then made into electrodes using both the inventive method and the conventional method.

EXAMPLE 10: Preparation of two-dimensional (2D) layered Bi₂Se₃ chalcogenide nanoribbons

The preparation of (2D) layered Bi₂Se₃ chalcogenide nanoribbons is well-known in the art. For instance, Bi₂Se₃ nanoribbons were grown using the vapor-liquid-solid (VLS) method. Nanoribbons herein produced are, on average, 30-55 nm thick with widths and lengths ranging from hundreds of nanometers to several micrometers. Larger nanoribbons were subjected to ball-milling for reducing the lateral dimensions (length and width) to below 200 nm. Nanoribbons prepared by these procedures (with or without the presence of graphene sheets or exfoliated graphite flakes) were used as a supercapacitor electrode active material.

EXAMPLE 11: MXenes powder + chemically activated RGO

Selected MXenes, were produced by partially etching out certain elements from layered structures of metal carbides such as Ti₃AlC₂. For instance, an aqueous 1 M NH₄HF₂ was used at room temperature as the etchant for Ti₃AlC₂. Typically, MXene surfaces are terminated by O, OH, and/or F groups, which is why they are usually referred to as M_{n+1}X_nT_x, where M is an early transition metal, X is C and/or N, T represents terminating groups (O, OH, and/or F), n = 1, 2, or 3, and x is the number of terminating groups. The MXene materials investigated include Ti₂CT_x, Nb₂CT_x, V₂CT_x, Ti₃CNT_x, and Ta₄C₃T_x. Typically, 35-95% MXene and 5-65% graphene sheets were mixed with a liquid electrolyte to form gel-like layers and stacked with conductive porous layers (stainless steel foam and graphite foam).

EXAMPLE 12: Preparation of MnO₂-graphene redox pairs

The MnO₂ powder was synthesized by two methods (each with or without the presence of graphene sheets). In one method, a 0.1 mol/L KMnO₄ aqueous solution was prepared by dissolving potassium permanganate in deionized water. Meanwhile 13.32 g surfactant of high purity sodium bis(2-ethylhexyl) sulfosuccinate was added in 300mL iso-octane (oil) and stirred

well to get an optically transparent solution. Then, 32.4mL of 0.1 mol/L KMnO₄ solution and selected amounts of GO solution were added in the solution, which was ultrasonicated for 30 min to prepare a dark brown precipitate. The product was separated, washed several times with distilled water and ethanol, and dried at 80°C for 12 h. The sample is graphene-supported MnO₂ in a powder form, which was mixed with a liquid electrolyte to form electrolyte-active material layers.

EXAMPLE 13: Evaluation of various supercapacitor cells

In most of the examples investigated, both the inventive supercapacitor cells and their conventional counterparts were fabricated and evaluated. The latter cells, for comparison purposes, were prepared by the conventional procedures of slurry coating of electrodes, drying of electrodes, assembling of anode layer, separator, and cathode layer, packaging of assembled laminate, and injection of liquid electrolyte. In a conventional cell, an electrode (cathode or anode), is typically composed of 85 % an electrode active material (e.g. graphene, activated carbon, inorganic nano discs, etc.), 5 % Super-P (acetylene black-based conductive additive), and 10 % PTFE, which were mixed and coated on Al foil. The thickness of electrode is around 100 µm. For each sample, both coin-size and pouch cells were assembled in a glove box. The capacity was measured with galvanostatic experiments using an Arbin SCTS electrochemical testing instrument. Cyclic voltammetry (CV) and electrochemical impedance spectroscopy (EIS) were conducted on an electrochemical workstation (CHI 660 System, USA).

Galvanostatic charge/discharge tests were conducted on the samples to evaluate the electrochemical performance. For the galvanostatic tests, the specific capacity (*q*) is calculated as

$$q = I*t/m \quad (1)$$

where *I* is the constant current in mA, *t* is the time in hours, and *m* is the cathode active material mass in grams. With voltage *V*, the specific energy (*E*) is calculated as,

$$E = \int V dq \quad (2)$$

The specific power (*P*) can be calculated as

$$P = (E/t) (W/kg) \quad (3)$$

where *t* is the total charge or discharge step time in hours.

The specific capacitance (C) of the cell is represented by the slope at each point of the voltage vs. specific capacity plot,

$$C = dq/dV \quad (4)$$

For each sample, several current density (representing charge/discharge rates) were imposed to determine the electrochemical responses, allowing for calculations of energy density and power density values required of the construction of a Ragone plot (power density vs. energy density).

Shown in FIG.5 are Ragone plots (gravimetric and volumetric power density vs. energy density) of two sets of symmetric supercapacitor (EDLC) cells containing reduced graphene oxide (RGO) sheets as the electrode active material and EMIMBF4 ionic liquid as the electrolyte. One of the two series of supercapacitors was prepared according to an embodiment of instant invention and the other was by the conventional method of slurry coating, drying, laminating (to form a cell), and liquid electrolyte injection into the cell. Several significant observations can be made from these data:

- (A) Both the gravimetric and volumetric energy densities and power densities of the supercapacitor cells prepared by the presently invented method (denoted as “inventive” in the figure legend) are significantly higher than those of their counterparts prepared via the conventional method (denoted as “conventional”). The differences are highly dramatic and are mainly due to the high active material mass loading ($> 20 \text{ mg/cm}^2$) associated with the presently invented cells, reduced proportion of overhead (non-active) components relative to the active material weight/volume, no need to have a binder resin, the ability of the inventive method to more effectively pack graphene sheets into pores of the foamed current collector.
- (B) For the cells prepared by the conventional method, the absolute magnitudes of the volumetric energy densities and volumetric power densities are significantly lower than those of their gravimetric energy densities and gravimetric power densities, due to the very low tap density (packing density of 0.25 g/cm^3) of RGO-based electrodes prepared by the conventional slurry coating method.

(C) In contrast, for the cells prepared by the presently invented method, the absolute magnitudes of the volumetric energy densities (27.4 Wh/L) and volumetric power densities (10,155 W/L) are higher than those of their gravimetric energy densities and gravimetric power densities, due to the relatively high tap density (packing density of 1.15 g/cm³) of RGO-based electrodes prepared by the presently invented method.

(D) The volumetric energy densities and volumetric power densities of corresponding supercapacitors prepared by the conventional process are 3.1 Wh/L and 1,139 W/L, respectively, which are one order of magnitude lower. These are dramatic and unexpected.

Figure 6 shows the Ragone plots (both gravimetric and volumetric power density vs. energy density) of symmetric supercapacitor (EDLC) cells containing activated carbon (AC) particles as the electrode active material and organic liquid electrolyte. The experimental data were obtained from the supercapacitors that were prepared by the presently invented method and those by the conventional slurry coating of electrodes.

These data also indicate that both the gravimetric and volumetric energy densities and power densities of the supercapacitor cells prepared by the presently invented method are significantly higher than those of their counterparts prepared via the conventional method. Again, the differences are huge and are mainly due to the high active material mass loading (> 15 mg/cm²) associated with the presently invented cells, reduced proportion of overhead (non-active) components relative to the active material weight/volume, no need to have a binder resin, the ability of the inventive method to more effectively pack graphene sheets into pores of the foamed current collectors. The highly porous activated carbon particles are not as amenable to more compact packing as graphene sheets. Consequently, for AC-based supercapacitors, the absolute magnitudes of the volumetric energy densities and volumetric power densities are lower than those of corresponding gravimetric energy densities and gravimetric power densities. However, the presently invented methods still surprisingly enables the AC particles to be packed with a significantly higher tap density (0.75 g/cm³) than what is achieved with the conventional slurry coating process (0.55 g/cm³) in the present study.

Shown in FIG. 7(A) are Ragone plots of lithium ion capacitor (LIC) cells containing pristine graphene sheets as the cathode active material, prelithiated graphite particles as the anode active material, and lithium salt (LiPF₆)-PC/DEC solvent as organic liquid electrolyte. The data are for both LICs prepared by the presently invented method and those by the conventional slurry coating of electrodes. These data indicate that both the gravimetric and volumetric energy densities and power densities of the LIC cells prepared by the presently invented method are significantly higher than those of their counterparts prepared via the conventional method. Again, the differences are huge and are mainly ascribed to the high active material mass loading (> 15 mg/cm² at the anode side and > 25 mg/cm² at the cathode side) associated with the presently invented cells, reduced proportion of overhead (non-active) components relative to the active material weight/volume, no need to have a binder resin, the ability of the inventive method to more effectively pack graphene sheets into pores of the foamed current collectors.

For the LIC cells prepared by the conventional method, the absolute magnitudes of the volumetric energy densities and volumetric power densities are significantly lower than those of their gravimetric energy densities and gravimetric power densities, due to the very low tap density (packing density of 0.25 g/cm³) of pristine graphene-based cathodes prepared by the conventional slurry coating method. In contrast, for the LIC cells prepared by the instant method, the absolute magnitudes of the volumetric energy densities and volumetric power densities are higher than those of their gravimetric energy densities and gravimetric power densities, due to the relatively high tap density of pristine graphene-based cathodes prepared by the presently invented method.

Shown in FIG. 7(B) are Ragone plots of sodium-ion capacitor (NIC) cells containing pristine graphene sheets as the cathode active material, pre-sodiated graphite particles as the anode active material, and sodium salt (NaPF₆)-PC/DEC as organic liquid electrolyte. The data are for both LICs prepared by the presently invented method and those by the conventional slurry coating of electrodes. These data indicate that both the gravimetric and volumetric energy densities and power densities of the NIC cells prepared by the presently invented method are significantly higher than those of their counterparts prepared via the conventional method. Again, the differences are dramatic and are mainly due to the high active material mass loading

($> 15 \text{ mg/cm}^2$ at the anode side and $> 25 \text{ mg/cm}^2$ at the cathode side) associated with the presently invented cells, reduced proportion of overhead (non-active) components relative to the active material weight/volume, no need to have a binder resin, the ability of the inventive method to more effectively pack graphene sheets into pores of the foamed current collectors.

It is of significance to point out that reporting the energy and power densities per weight of active material alone on a Ragone plot, as did by many researchers, may not give a realistic picture of the performance of the assembled supercapacitor cell. The weights of other device components also must be taken into account. These overhead components, including current collectors, electrolyte, separator, binder, connectors, and packaging, are non-active materials and do not contribute to the charge storage amounts. They only add weights and volumes to the device. Hence, it is desirable to reduce the relative proportion of overhead component weights and increase the active material proportion. However, it has not been possible to achieve this objective using conventional supercapacitor production processes. The present invention overcomes this long-standing, most serious problem in the art of supercapacitors.

In a commercial supercapacitor having an electrode thickness of 150-200 μm (75-100 μm on each side of an Al foil current collector), the weight of the active material (i.e. activated carbon) accounts for about 25%-30% of the total mass of the packaged cell. Hence, a factor of 3 to 4 is frequently used to extrapolate the energy or power densities of the device (cell) from the properties based on the active material weight alone. In most of the scientific papers, the properties reported are typically based on the active material weight alone and the electrodes are typically very thin ($<< 100 \mu\text{m}$, and mostly $<< 50 \mu\text{m}$). The active material weight is typically from 5% to 10% of the total device weight, which implies that the actual cell (device) energy or power densities may be obtained by dividing the corresponding active material weight-based values by a factor of 10 to 20. After this factor is taken into account, the properties reported in these papers do not really look any better than those of commercial supercapacitors. Thus, one must be very careful when it comes to read and interpret the performance data of supercapacitors reported in the scientific papers and patent applications.

EXAMPLE 14: Achievable electrode thickness and its effect on electrochemical performance of supercapacitor cells

One might be tempted to think the electrode thickness of a supercapacitor is a design parameter that can be freely adjusted for optimization of device performance; but, in reality, the supercapacitor thickness is manufacturing-limited and one cannot produce electrodes of good structural integrity that exceed certain thickness level. Our studies further indicate that this problem is even more severe with graphene-based electrode. The instant invention solves this critically important issue associated with supercapacitors.

Shown in FIG.8 are the cell-level gravimetric (Wh/kg) and volumetric energy densities (Wh/L) plotted over the achievable electrode thickness range of the activated carbon-based symmetric EDLC supercapacitors prepared via the conventional method and those by the presently invented method. In this figure, the data points are labelled as the gravimetric (♦) and volumetric (▲) energy density of the conventional supercapacitors and the gravimetric (■) and volumetric (X) energy density of the presently invented supercapacitors. The activated carbon-based electrodes can be fabricated up to a thickness of 100-200 μm using the conventional slurry coating process. However, in contrast, there is no theoretical limit on the electrode thickness that can be achieved with the presently invented method. Typically, the practical electrode thickness is from 10 μm to 5000 μm , more typically from 50 μm to 2,000 μm , further more typically from 100 μm to 1,000 μm , and most typically from 200 μm to 800 μm .

These data further confirm the surprising effectiveness of the presently invented method in producing ultra-thick supercapacitor electrodes not previously achievable. These ultra-thick electrodes lead to exceptionally high active material mass loading, typically significantly $> 10 \text{ mg/cm}^2$ (more typically $> 15 \text{ mg/cm}^2$, further typically $> 20 \text{ mg/cm}^2$, often $> 25 \text{ mg/cm}^2$, and even $> 30 \text{ mg/cm}^2$). These high active material mass loadings have not been possible to obtain with conventional supercapacitors made by the slurry coating processes.

Further significantly, the typical cell-level energy densities of commercial AC-based supercapacitors are from 3 to 8 Wh/kg and from 1 to 4 Wh/L. In contrast, the presently invented method enables supercapacitors containing the same type of electrode active material (AC) to deliver an energy density up to 25 Wh/kg or 20 Wh/L. Such an increase in energy density has not been considered possible in the supercapacitor industry.

Also highly significant and unexpected are the data summarized in FIG.9 for reduced graphene oxide-based EDLC supercapacitors. The cell-level gravimetric and volumetric energy

densities plotted over the achievable electrode thickness range of the RGO-based EDLC supercapacitors (organic liquid electrolyte) prepared via the conventional method and those by the presently invented method. In this figure, the gravimetric (♦) and volumetric (▲) energy density of the conventional supercapacitors are based on the highest achieved electrode tap density of approximately 0.25 g/cm³, and the gravimetric (■) and volumetric (X) energy density of the presently invented supercapacitors are from those having an electrode tap density of approximately 0.75 g/cm³, by no means the highest. No one else has previously reported such a high tap density for un-treated, non-activated RGO electrodes.

These data indicate that the highest gravimetric energy density achieved with RGO-based EDLC supercapacitor cells produced by the conventional slurry coating method is approximately 12 Wh/kg, but those prepared by the presently invented method exhibit a gravimetric energy density as high as 31.6 Wh/kg at room temperature. This is an unprecedentedly high energy density value for EDLC supercapacitors (based on the total cell weight, not the electrode weight or active material weight alone). Even more impressive is the observation that the volumetric energy density of the presently invented supercapacitor cell is as high as 23.7 Wh/L, which is more than 7 times greater than the 3.0 Wh/L achieved by the conventional counterparts.

Summarized in FIG.10 are the data of the cell-level gravimetric and volumetric energy densities plotted over the achievable electrode thickness range of the pristine graphene-based EDLC supercapacitors (organic liquid electrolyte) prepared via the conventional method and those by the presently invented method. The legends include the gravimetric (♦) and volumetric (▲) energy density of the conventional supercapacitors (highest achieved electrode tap density of approximately 0.25 g/cm³) and the gravimetric (■) and volumetric (X) energy density of the presently invented supercapacitors (electrode tap density of approximately 1.15 g/cm³).

Quite significantly, these EDLC supercapacitors (without any redox or pseudo-capacitance) deliver a gravimetric energy density as high as 43.9 Wh/kg, which already exceeds the energy densities (20-40 Wh/kg) of advanced lead-acid batteries. This is of high utility value since an EDLC supercapacitor can be charged and discharged for 250,000-500,000 cycles, as opposed to the typical 100-400 cycles of lead-acid batteries. This achievement is very dramatic and totally unexpected in the art of supercapacitors. In addition, carbon- or graphene-based EDLC supercapacitors can be re-charged in seconds, in contrast to the typically hours of

recharge time required of lead-acid batteries. Lead-acid batteries are notorious for their highly negative environmental impact, yet the instant supercapacitors are environmentally benign.

Further significant examples include those data summarized in FIG.11 for the cell-level gravimetric and volumetric energy densities plotted over the achievable electrode thickness range of the pristine graphene-based EDLC supercapacitors (ionic liquid electrolyte) prepared via the conventional method and those via the presently invented method. The gravimetric (♦) and volumetric (▲) energy density are for those conventional supercapacitors (highest achieved electrode tap density of approximately 0.25 g/cm³, more typically < 0.1 g/cm³) and the gravimetric (■) and volumetric (X) energy density are for those inventive supercapacitors having an electrode tap density of approximately 1.15 g/cm³. The presently invented pristine graphene-based EDLC supercapacitors are capable of storing a cell-level energy density of 97.7 Wh/kg, which is 15 times greater than what could be achieved by conventional AC-based EDLC supercapacitors. The volumetric energy density value of 112.3 Wh/L is also unprecedented and is 30-fold greater than the 3-4 Wh/L of commercial AC-based supercapacitors.

EXAMPLE 15: Achievable active material weight percentage in a cell and its effect on electrochemical performance of supercapacitor cells

Because the active material weight accounts for up to about 30% of the total mass of the packaged commercial supercapacitors, a factor of 30% must be used to extrapolate the energy or power densities of the device from the performance data of the active material alone. Thus, the energy density of 20 Wh/kg of activated carbon (i.e. based on the active material weight alone) will translate to about 6 Wh/kg of the packaged cell. However, this extrapolation is only valid for electrodes with thicknesses and densities similar to those of commercial electrodes (150 µm or about 10 mg/cm² of the carbon electrode). An electrode of the same active material that is thinner or lighter will mean an even lower energy or power density based on the cell weight. Thus, it would be desirable to produce a supercapacitor cell having a high active material proportion. Unfortunately, it has not been previously possible to achieve an active material proportion greater than 30% by weight for activated carbon-based supercapacitors or greater than 15% by weight for graphene-based supercapacitors.

The presently invented method enables the supercapacitors to go well beyond these limits for all active materials investigated. As a matter of fact, the instant invention makes it possible to elevate the active material proportion above 90% if so desired; but typically from 15% to 85%, more typically from 30% to 80%, even more typically from 40% to 75%, and most typically from 50% to 70%.

As shown in FIG.12, the cell-level gravimetric energy densities of the activated carbon-based EDLC supercapacitors (with organic liquid electrolyte) are plotted over the achievable active material proportion (active material weight/total cell weight), which are from 17.5% to 75.4%. The instant invention also allows us to achieve a pristine graphene content in a supercapacitor cell from 9.6% to 78.2% by weight, resulting in a gravimetric energy density from 9.6 Wh/kg to 97.7 Wh/kg. For instance, FIG.13 shows the cell-level gravimetric energy densities plotted over the achievable active material proportion (active material weight/total cell weight) in a supercapacitor cell for two series of pristine graphene-based EDLC supercapacitors (all with organic liquid electrolyte). FIG.14 shows the cell-level volumetric energy densities plotted over the achievable active material proportion (active material weight/total cell weight) for pristine graphene-based EDLC supercapacitors (with ionic liquid electrolyte).

EXAMPLE 16: The electrochemical performance of supercapacitor cells based on various electrode active materials and/or different porous or foamed structures as current collectors

In order to evaluate the effect of the foam structure, we chose to use RGO as an example of electrode active material but vary the type and nature of the current collector. A wide variety of foams were selected, ranging from metal foam (e.g. Ni and Ti foam), metal web or screen (e.g. stainless steel web), perforated metal sheet-based 3-D structure, metal fiber mat (steel fibers), metal nanowire mat (Cu nanowires), conductive polymer nano-fiber mat (polyaniline), conductive polymer foam (e.g. PEDOT), conductive polymer-coated fiber foam (polypyrrole-coated nylon fibers), carbon foam, graphite foam, carbon aerogel, carbon xerox gel, graphene foam (from Ni-supported CVD graphene), graphene oxide foam (obtained via freeze-drying GO-water solution), reduced graphene oxide foam (RGO mixed with a polymer and then carbonized), carbon fiber foam, graphite fiber foam, and exfoliated graphite foam (exfoliated

graphite worms bonded by a carbonized resin). This extensive and in-depth study leads to the following important observations:

- (A) The electrical conductivity of the foam material is an important parameter with a higher conductivity tending to result in a higher power density and faster supercapacitor response time.
- (B) The porosity level is also an important parameter with a higher pore content resulting in a larger amount of active material given the same volume, leading to a higher energy density. However, a higher porosity level can lead to slower response time possibly due to a lower electron-conducting capability.
- (C) Graphite foams and graphene foams provide better response time of a supercapacitor. However, metal foam enables more ready formation of or connection to a tab (terminal lead). Two leads are required in each cell.

A wide variety of electrode active materials for both EDLC and redox supercapacitors have been investigated, covering organic and inorganic materials, in combination with aqueous, organic, and ionic liquid electrolytes. Summarized in the following table (Table 1) are some examples of different classes of supercapacitors for illustration purposes. These should not to be construed as limiting the scope of the instant application.

Table 1: Examples of supercapacitors prepared by the new method and their counterparts prepared by the conventional slurry coating method.

Sample ID	Active materials	Electrolyte	Electrode thickness (μm) and method	Active mass loading (g/cm^2)	Gravimetric energy density (Wh/kg)	Volumetric energy density (Wh/L)
PPy-1	Polypyrrole-cellulose	2 M NaCl in H_2O	530, new	39	41	20
PPy-c	Polypyrrole-cellulose	2 M NaCl in H_2O	190, conventional	13.2	8.8	3.1
RuO ₂ -AC-1	RuO ₂ + AC	1 M NaCl in H_2O	365, new	16.6	37.9	26.8
RuO ₂ -AC-c	RuO ₂ + AC	1 M NaCl in H_2O	160, conventional	7.2	11.6	7.7
NiO-RGO-1	NiO + activated GO	1 M LiOH in H_2O	555, new	26.7	44.5	35.8
NiO-RGO-c	NiO + Activated GO	1 M LiOH in H_2O	160, conventional	4.6	9.2	7.3
V ₂ O ₅ -NGn-1	V ₂ O ₅ +	THF +	629, new	27.5	41.6	35.6

	nitrogenated graphene	N(Et) ₄ BF ₄				
V ₂ O ₅ -NGn-c	V ₂ O ₅ + nitrogenated graphene	THF + N(Et) ₄ BF ₄	175, conventional	5.6	7.2	5.6
MnO ₂ -RGO -1	MnO ₂ + RGO	1.0 M Na ₂ SO ₄	430, new	17.7	86	85
MnO ₂ -RGO -c	MnO ₂ + RGO	1.0 M Na ₂ SO ₄	187, conventional	6.2	29	23
MoS ₂ -1	MoS ₂ /RGO	Acetonitrile +N(Et) ₄ BF ₄	385, new	26.8	43.4	36.4
MoS ₂ -c	MoS ₂ /RGO	Acetonitrile N(Et) ₄ BF ₄	155, conventional	8.8	13.2	9.6
Ti ₂ CT _x -1	Ti ₂ C(OH) ₂ / quinone GO	1 M LiOH in H ₂ O	334, new	15.7	15.9	12.9
Ti ₂ CT _x -c	Ti ₂ C(OH) ₂ / quinone GO	1 M LiOH in H ₂ O	167, conventional	4.5	6.7	4.2
CNT-1	MWCNT	EMI-TFSI	275	12.7	25.8	16.7
CNT-c	MWCNT	EMI-TFSI	95	2.3	6.2	3.2

These data further confirm the surprising superiority of the presently invented method of producing supercapacitor cells in terms of dramatically improving mass loading, electrode thickness, gravimetric energy density, and volumetric energy density. The presently invented supercapacitors are consistently much better the conventional supercapacitors in electrochemical properties. The differences are surprisingly dramatic.

In conclusion, we have successfully developed a new and novel class of supercapacitors that have unexpectedly thick electrodes (not previously achievable), large active material mass loading (not previously achievable), outstanding gravimetric energy density (not previously achievable), and unprecedently high volumetric energy density. The invented method of alternately stacking active material-electrolyte mixture layers with foamed current collector layers also overcomes the long-standing problems associated with graphene sheet-based supercapacitors (i.e. inability to make thick electrodes, difficulty in preventing graphene sheet re-stacking, low tap density, and low volumetric energy density).

We claim:

1. A process for producing a supercapacitor cell, said process comprising:
 - (A) Preparing a plurality of electrically conductive porous layers, a plurality of wet anode layers of an anode active material and an optional conductive additive mixed with a first liquid or gel electrolyte, and a plurality of wet cathode layers of a cathode active material and an optional conductive additive mixed with a second liquid or gel electrolyte, wherein said conductive porous layers contain interconnected conductive pathways and at least 80% by volume of pores;
 - (B) Stacking and consolidating a desired number of said porous layers and a desired number of said wet anode layers to form an anode electrode having a thickness no less than 100 μm ;
 - (C) Placing a porous separator layer in contact with said anode electrode;
 - (D) Stacking and consolidating a desired number of said porous layers and a desired number of said wet cathode layers to form a cathode electrode in contact with said porous separator, wherein said cathode electrode has a thickness no less than 100 μm ; wherein said step (d) is conducted before or after step (B); and
 - (E) Assembling and sealing said anode electrode, porous separator, and cathode electrode in a housing to produce said supercapacitor cell; wherein said anode electrode and/or said cathode electrode has a material mass loading no less than 7 mg/cm^2 .
2. The process of claim 1, wherein said anode active material and/or said cathode active material contains multiple particles of a carbon material and/or multiple graphene sheets, wherein said multiple graphene sheets contain single-layer graphene or few-layer graphene each having from 1 to 10 graphene planes and said multiple particles of carbon material have a specific surface area no less than 500 m^2/g when measured in a dried state.
3. A process for producing an electrode for a supercapacitor cell, said process comprising:
 - (a) Preparing a plurality of electrically conductive porous layers and a plurality of wet electrode layers composed of an electrode active material and an optional conductive

additive mixed with a liquid or gel electrolyte, wherein said conductive porous layers contain interconnected conductive pathways and at least 80% by volume of pores; and

- (b) Stacking and consolidating a desired number of said porous layers and a desired number of said wet electrode layers to form an electrode having a thickness no less than 100 μm .
- 4. The process of claim 3, wherein said electrode active material contains multiple particles of a carbon material and/or multiple graphene sheets, wherein said multiple graphene sheets contain single-layer graphene or few-layer graphene each having from 1 to 10 graphene planes and said multiple particles of carbon material have a specific surface area no less than 500 m^2/g when measured in a dried state.
- 5. The process of claim 3, wherein said electrode is a cathode electrode and said process further contains (c) supplying an anode electrode, which contains a pre-lithiated or pre-sodiated anode active material; and (d) stacking the anode electrode, a porous separator, and the cathode electrode to form a lithium-ion capacitor or sodium-ion capacitor.
- 6. The process of claim 1, wherein said electrically conductive porous layer has a thickness no less than 200 μm , has at least 85% by volume of pores, and/or said electrode active material loading is no less than 10 mg/cm^2 .
- 7. The process of claim 1, wherein said electrically conductive porous layer has a thickness no less than 300 μm , has at least 90% by volume of pores, and/or said electrode active material loading is no less than 15 mg/cm^2 .
- 8. The process of claim 1, wherein said electrically conductive porous layer has a thickness no less than 400 μm , has at least 95% by volume of pores, and/or said electrode active material loading is no less than 20 mg/cm^2 .
- 9. The process of claim 1, wherein said electrically conductive porous layer is selected from metal foam, metal web or screen, perforated metal sheet-based 3-D structure, metal fiber mat, metal nanowire mat, conductive polymer nano-fiber mat, conductive polymer foam, conductive polymer-coated fiber foam, carbon foam, graphite foam, carbon aerogel, carbon xerox gel, graphene foam, graphene oxide foam, reduced graphene oxide foam, carbon fiber foam, graphite fiber foam, exfoliated graphite foam, or a combination thereof.

10. The process of claim 2, wherein said graphene sheets are selected from the group consisting of pristine graphene, graphene oxide, reduced graphene oxide, graphene fluoride, graphene chloride, graphene bromide, graphene iodide, hydrogenated graphene, nitrogenated graphene, boron-doped graphene, nitrogen-doped graphene, chemically functionalized graphene, physically or chemically activated or etched versions thereof, and combinations thereof.
11. The process of claim 4, wherein said graphene sheets are selected from the group consisting of pristine graphene, graphene oxide, reduced graphene oxide, graphene fluoride, graphene chloride, graphene bromide, graphene iodide, hydrogenated graphene, nitrogenated graphene, boron-doped graphene, nitrogen-doped graphene, chemically functionalized graphene, physically or chemically activated or etched versions thereof, and combinations thereof.
12. The process of claim 1, wherein said anode active material or cathode active material is selected from (a) graphene sheets alone; (b) graphene sheets mixed with a carbon material; (c) graphene sheets mixed with a partner material that forms a redox pair with said graphene sheets to develop pseudo-capacitance; or (d) graphene sheets and a carbon material mixed with a partner material that forms a redox pair with said graphene sheets or said carbon material to develop pseudo-capacitance, and wherein there is no other anode active material in said anode electrode and no other cathode active material in said cathode electrode.
13. The process of claim 1, wherein a volume ratio of said anode active material-to-said electrolyte in said wet anode layer is from 1/5 to 20/1 and/or a volume ratio of said cathode active material-to-said electrolyte in said wet cathode layer is from 1/5 to 20/1.
14. The process of claim 1, wherein a volume ratio of said anode active material-to-said electrolyte in said wet anode layer is from 1/3 to 5/1 and/or a volume ratio of said cathode active material-to-said electrolyte in said wet cathode layer is from 1/3 to 5/1.
15. The process of claim 2, wherein said anode active material or cathode active material further contains a redox pair partner material selected from a metal oxide, a conducting polymer, an organic material, a non-graphene carbon material, an inorganic material, or a combination thereof, wherein said partner material, in combination with graphene or a carbon material, form a redox pair for pseudo-capacitance.

16. The process of claim 4, wherein said anode active material or cathode active material further contains a redox pair partner material selected from a metal oxide, a conducting polymer, an organic material, a non-graphene carbon material, an inorganic material, or a combination thereof, wherein said partner material, in combination with graphene or a carbon material, form a redox pair for pseudo-capacitance.
17. The process of claim 15, wherein said metal oxide is selected from RuO₂, IrO₂, NiO, MnO₂, VO₂, V₂O₅, V₃O₈, TiO₂, Cr₂O₃, Co₂O₃, Co₃O₄, PbO₂, Ag₂O, or a combination thereof.
18. The process of claim 15, wherein said inorganic material is selected from a metal carbide, metal nitride, metal boride, metal dichalcogenide, or a combination thereof.
19. The process of claim 16, wherein said metal oxide or inorganic material is selected from an oxide, dichalcogenide, trichalcogenide, sulfide, selenide, or telluride of niobium, zirconium, molybdenum, hafnium, tantalum, tungsten, titanium, vanadium, chromium, cobalt, manganese, iron, or nickel in a nanowire, nano-disc, nano-ribbon, or nano platelet form.
20. The process of claim 15, wherein said inorganic material is selected from nano discs, nano platelets, nano-coating, or nano sheets of an inorganic material selected from: (a) bismuth selenide or bismuth telluride, (b) transition metal dichalcogenide or trichalcogenide, (c) sulfide, selenide, or telluride of niobium, zirconium, molybdenum, hafnium, tantalum, tungsten, titanium, cobalt, manganese, iron, nickel, or a transition metal; (d) boron nitride, or (e) a combination thereof; wherein said discs, platelets, or sheets have a thickness less than 100 nm.
21. The process of claim 1, wherein said anode active material and/or said cathode active material contains nano discs, nano platelets, nano-coating, or nano sheets of an inorganic material selected from: (i) bismuth selenide or bismuth telluride, (ii) transition metal dichalcogenide or trichalcogenide, (iii) sulfide, selenide, or telluride of niobium, zirconium, molybdenum, hafnium, tantalum, tungsten, titanium, cobalt, manganese, iron, nickel, or a transition metal; (iv) boron nitride, or (v) a combination thereof, wherein said discs, platelets, coating, or sheets have a thickness less than 100 nm and a specific surface area no less than 200 m²/g when measured in a dried state.

22. The process of claim 21, wherein said anode active material or cathode active material further contains graphene sheets selected from pristine graphene, graphene oxide, reduced graphene oxide, graphene fluoride, graphene chloride, graphene bromide, graphene iodide, hydrogenated graphene, nitrogenated graphene, boron-doped graphene, nitrogen-doped graphene, chemically functionalized graphene, or a combination thereof.
23. The process of claim 21, wherein said anode active material or cathode active material further contains a redox pair partner material selected from a carbon material, a graphene material, a metal oxide, a conducting polymer, an organic material, or a combination thereof, wherein said partner material, in combination with said inorganic material, form a redox pair for obtaining pseudo-capacitance.
24. The process of claim 23, wherein said metal oxide is selected from RuO₂, IrO₂, NiO, MnO₂, VO_x, TiO₂, Cr₂O₃, Co₂O₃, Co₃O₄, PbO₂, Ag₂O, or a combination thereof.
25. The process of claim 2, wherein said carbon material is selected from activated carbon, activated meso-carbon micro beads, activated graphite, activated or chemically etched carbon black, activated hard carbon, activated soft carbon, carbon nanotube, carbon nano-fiber, activated carbon fiber, activated graphite fiber, exfoliated graphite worms, activated graphite worms, activated expanded graphite flakes, or a combination thereof.
26. The process of claim 4, wherein said carbon material is selected from activated carbon, activated meso-carbon micro beads, activated graphite, activated or chemically etched carbon black, activated hard carbon, activated soft carbon, carbon nanotube, carbon nano-fiber, activated carbon fiber, activated graphite fiber, exfoliated graphite worms, activated graphite worms, activated expanded graphite flakes, or a combination thereof.
27. The process of claim 1, wherein said first liquid electrolyte or said second liquid electrolyte is selected from an aqueous liquid, an organic liquid, an ionic liquid, or a mixture of an organic liquid and an ionic liquid.
28. The process of claim 1, wherein said anode active material is different than the cathode active material.

29. The process of claim 3, further comprising a step of supplying at least a protective film to cover said at least one porous surface to form a protected electrode.
30. The process of claim 1, wherein said anode active material or said cathode active material constitutes an electrode active material loading greater than 10 mg/cm^2 and/or wherein said anode electrode or cathode electrode has a thickness no less than $200 \mu\text{m}$.
31. The process of claim 3, wherein said anode or cathode active material loading is greater than 15 mg/cm^2 , said anode active material and said cathode active material combined exceeds 40% by weight of said supercapacitor cell, and/or said anode electrode or cathode electrode has a thickness no less than $300 \mu\text{m}$.
32. The process of claim 1, wherein said anode or cathode active material loading is greater than 20 mg/cm^2 , said anode active material and said cathode active material combined exceeds 50% by weight of said supercapacitor cell, and/or said anode electrode or cathode electrode has a thickness no less than $400 \mu\text{m}$.
33. The process of claim 3, wherein said anode active material and said cathode active material combined exceeds 60% by weight of said supercapacitor cell, and/or said anode electrode or cathode electrode has a thickness no less than $500 \mu\text{m}$.
34. A supercapacitor cell produced by the process of claim 1.
35. A supercapacitor cell produced by the process of claim 5, which is a lithium-ion capacitor or sodium-ion capacitor.

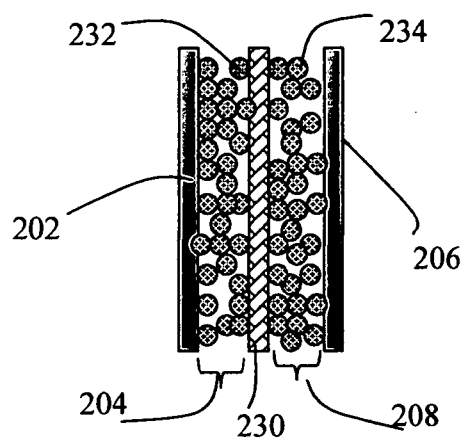


FIG. 1(A) Prior art

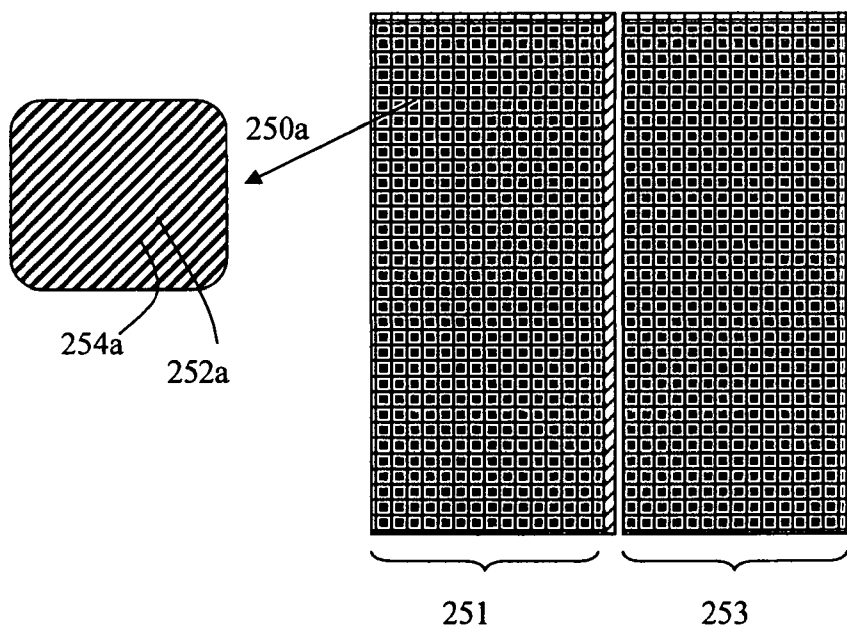


FIG. 1(B)

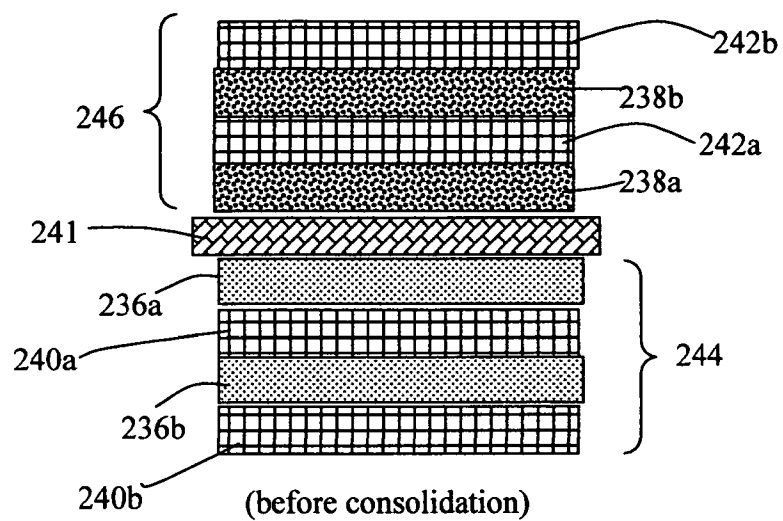


FIG. 1(C)

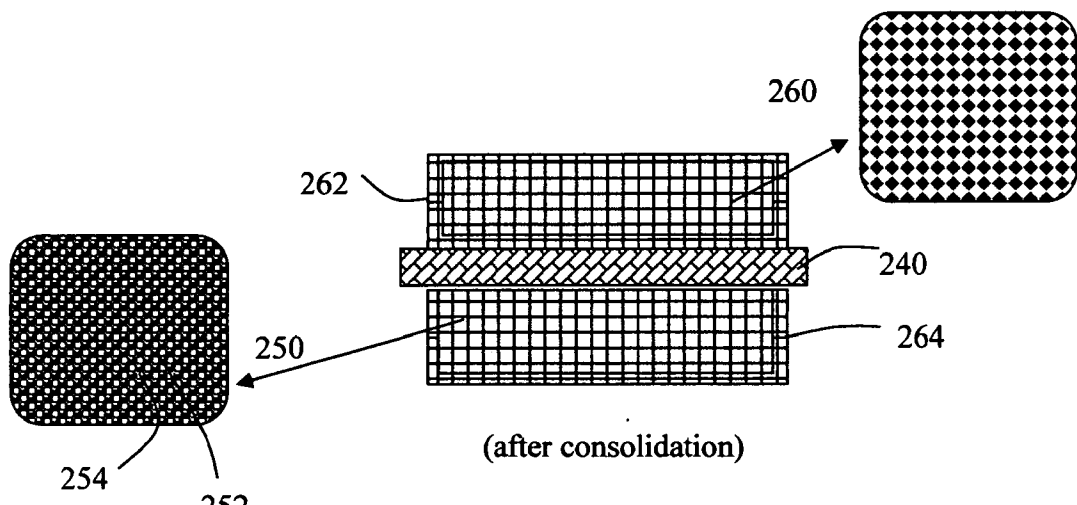


FIG. 1(D)

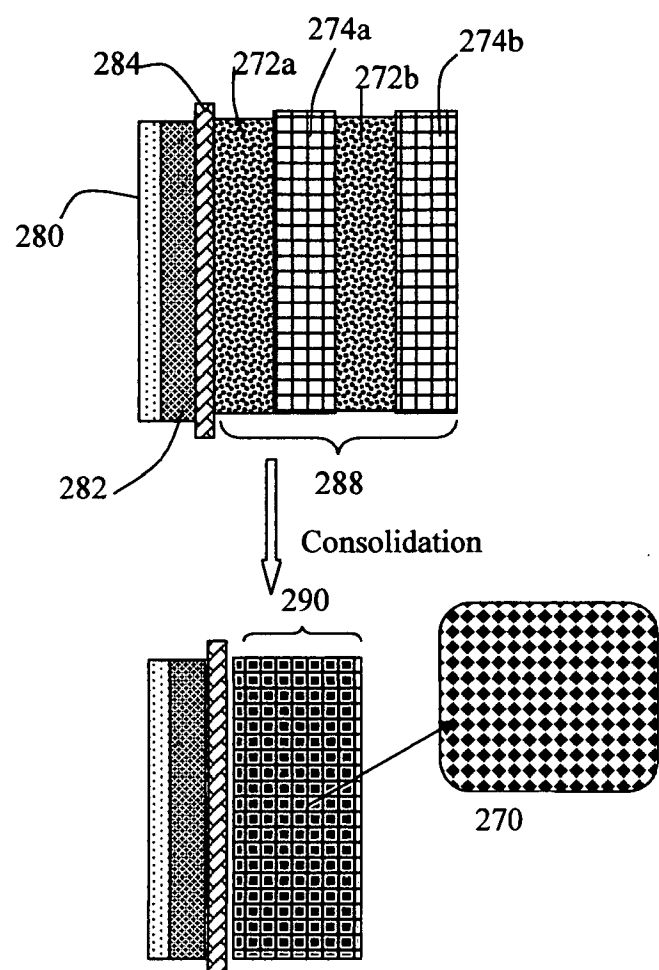
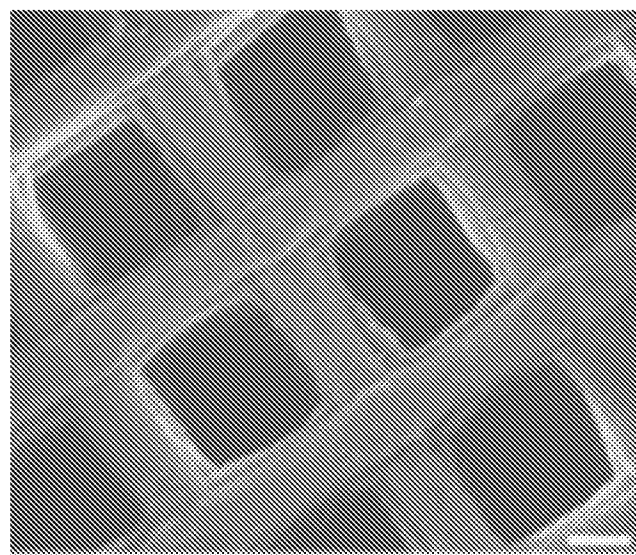


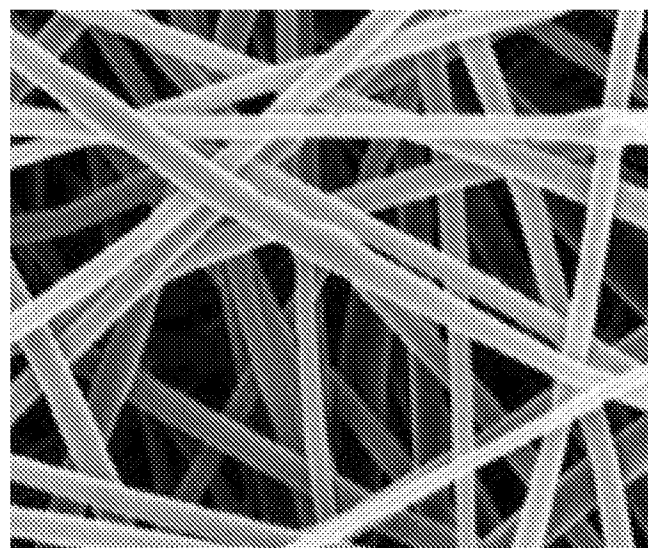
FIG. 1(E)



FIG. 2

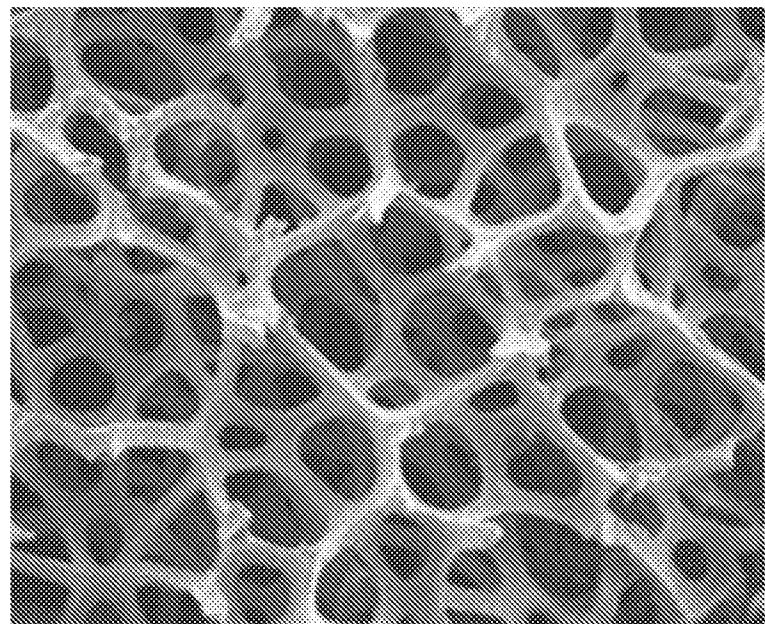


Metal grid; scale = 200 μm

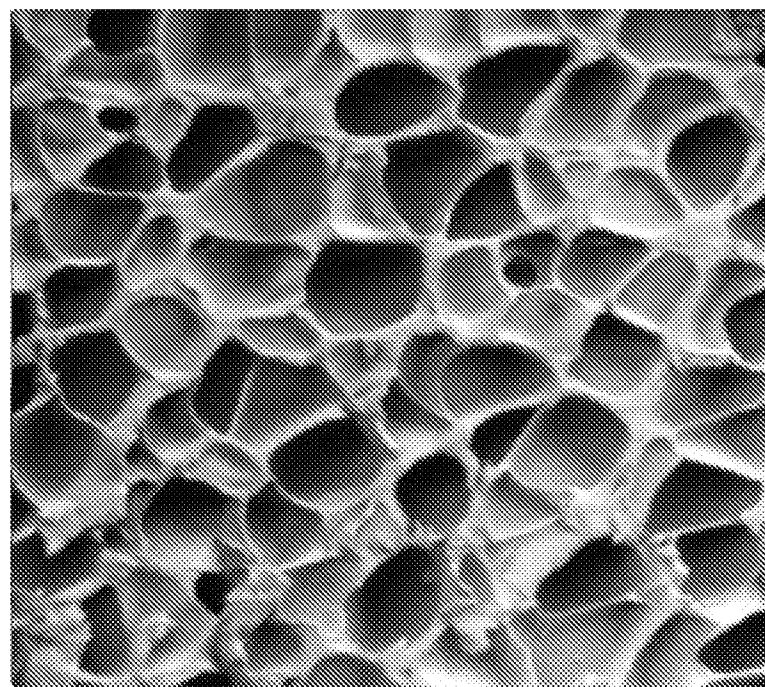


Carbon nano-fiber mat; fiber diameter = 150 nm

FIG. 3(A)

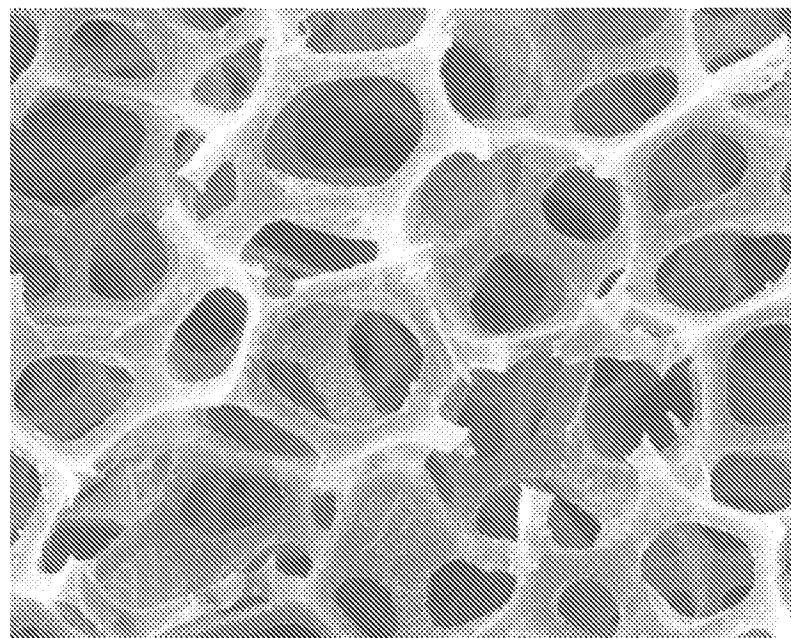


Graphene foam; 100 μm

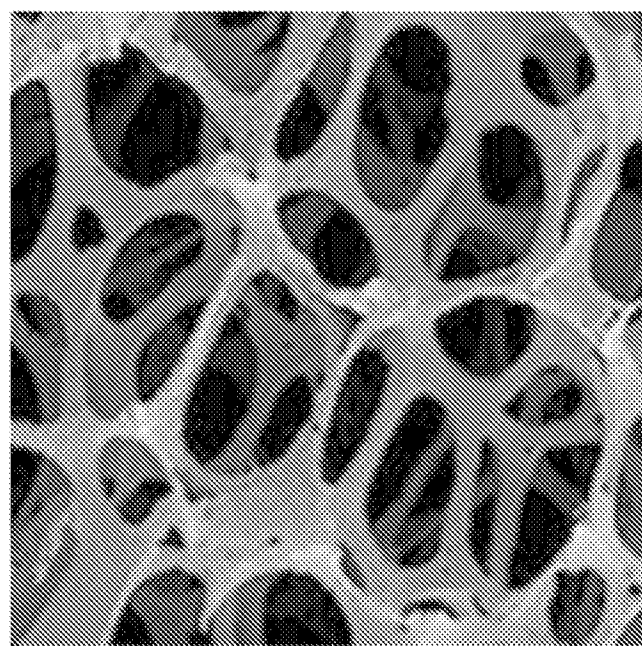


Carbon foam

FIG. 3(B)

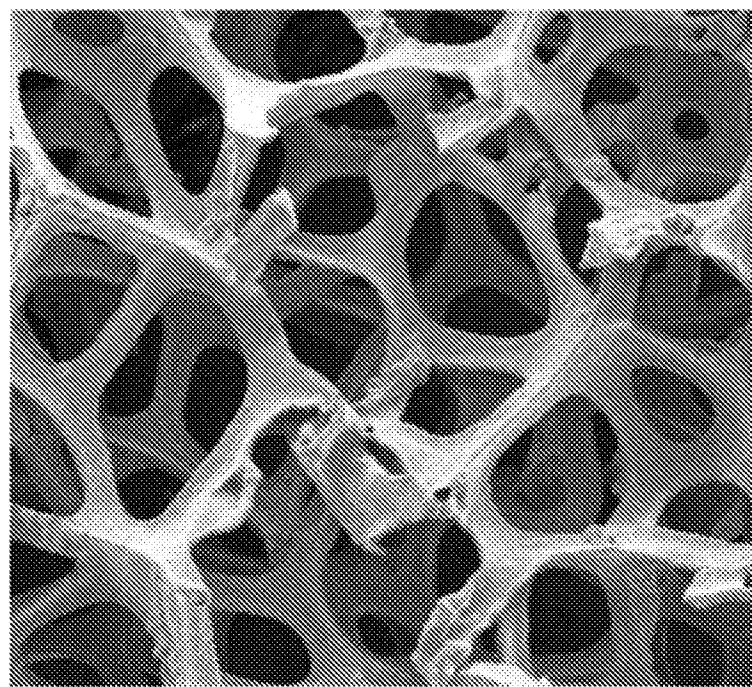


Graphite foam

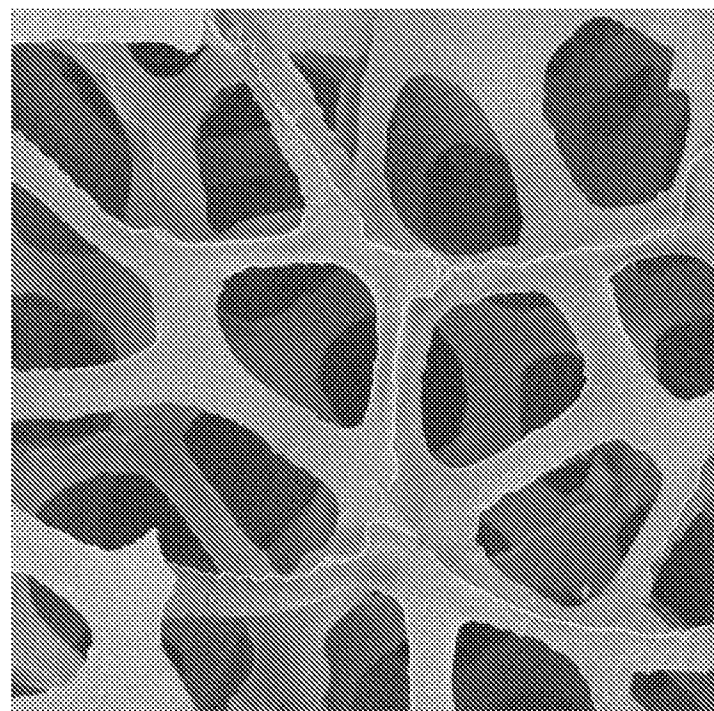


Ni foam

FIG. 3(C)

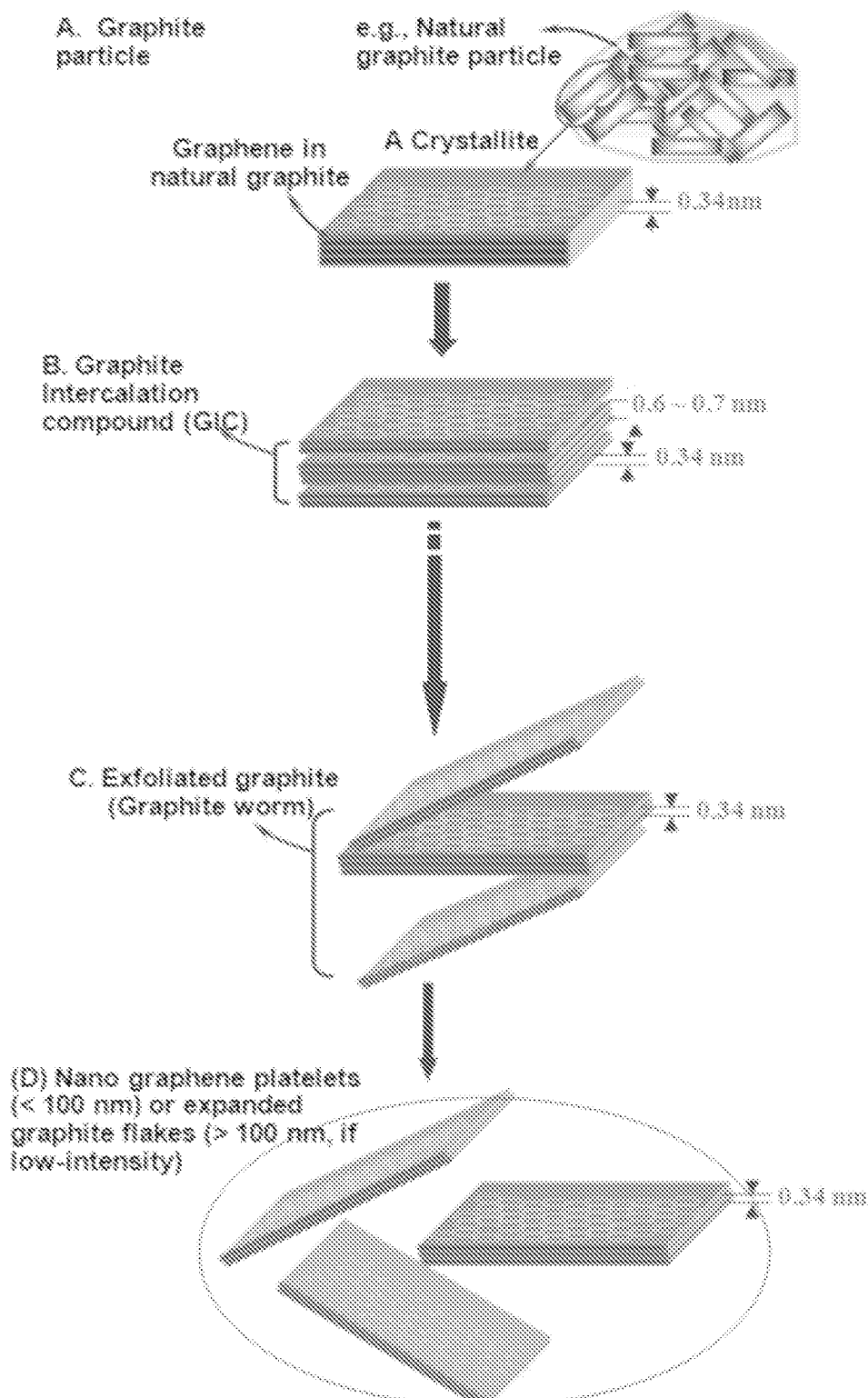


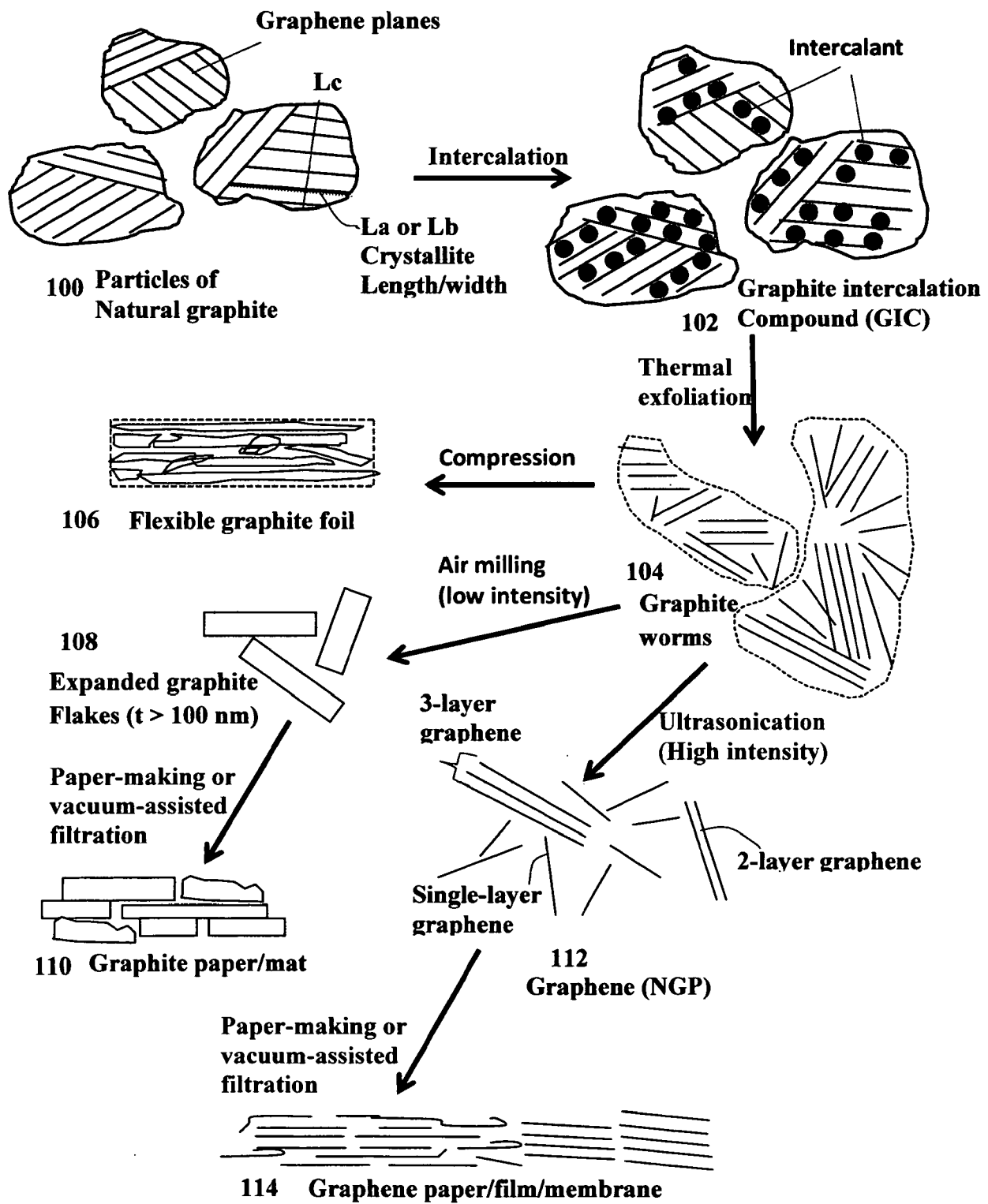
Cu foam

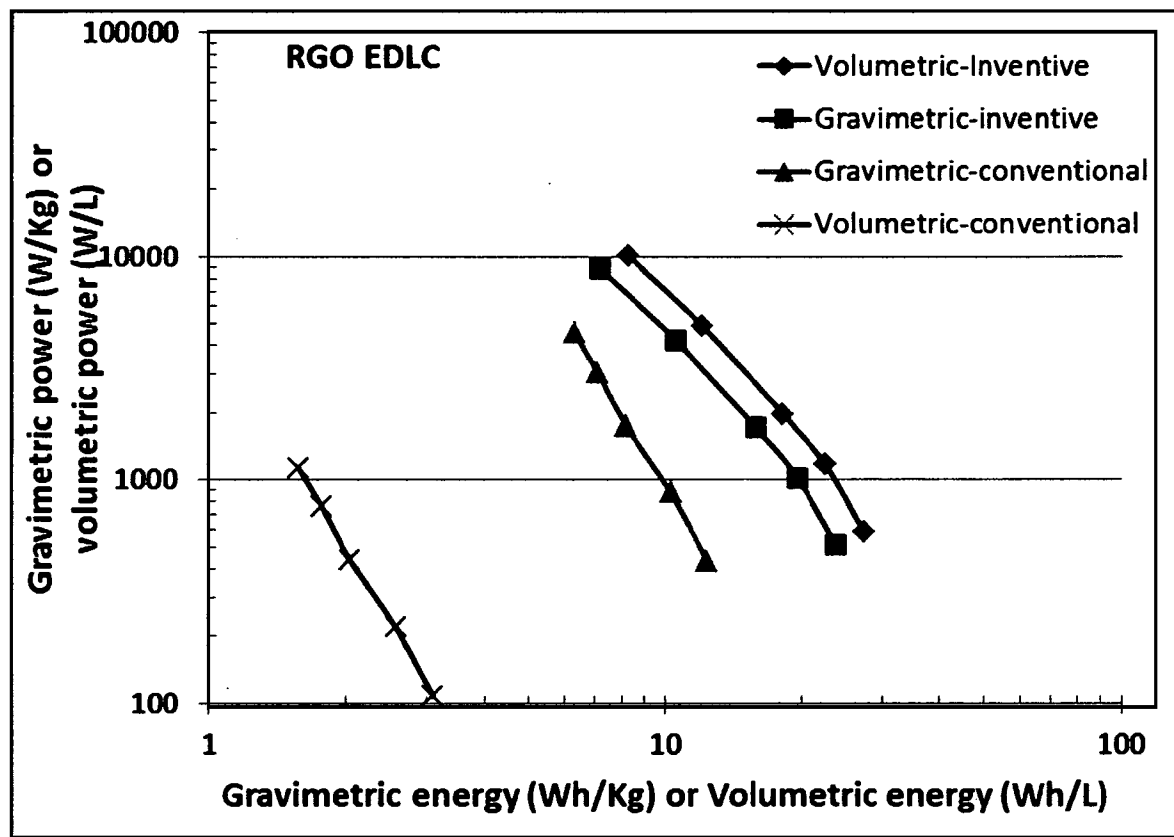


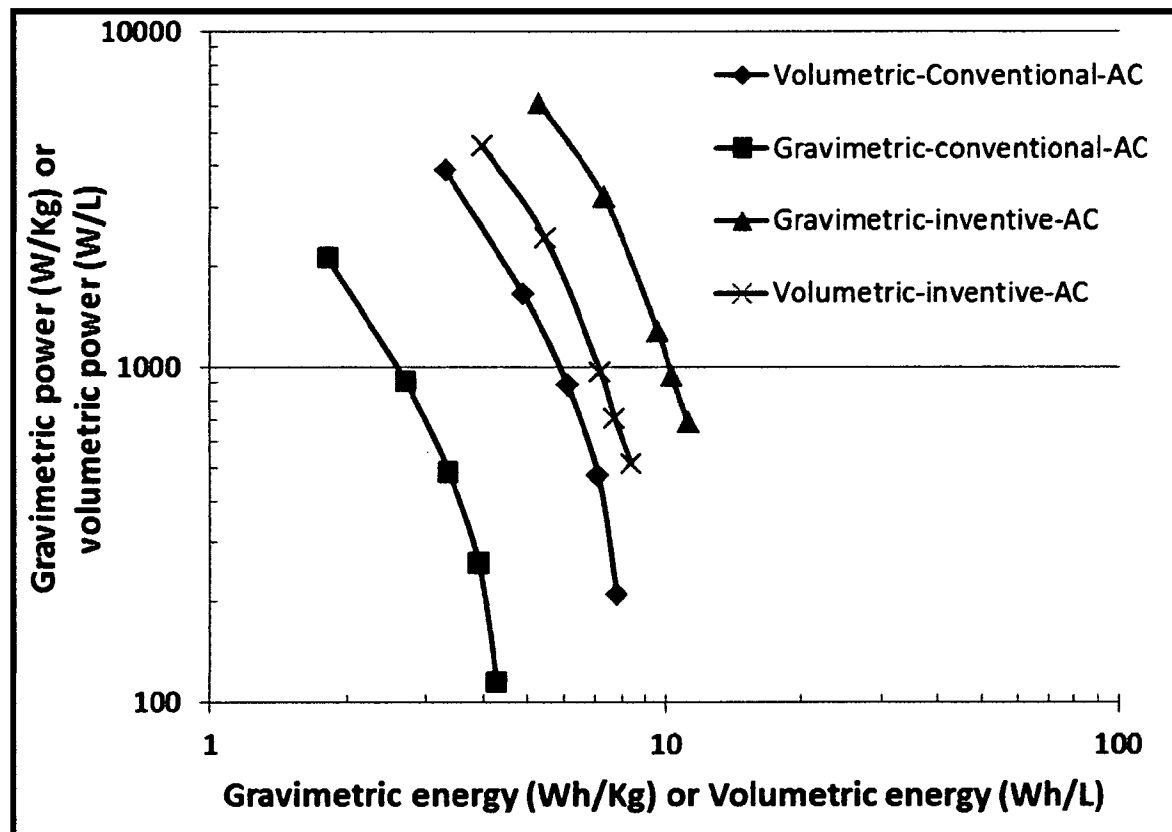
Stainless steel foam

FIG. 3(D)

**FIG. 4(A)**

**FIG. 4 (B)**

**FIG. 5**

**FIG. 6**

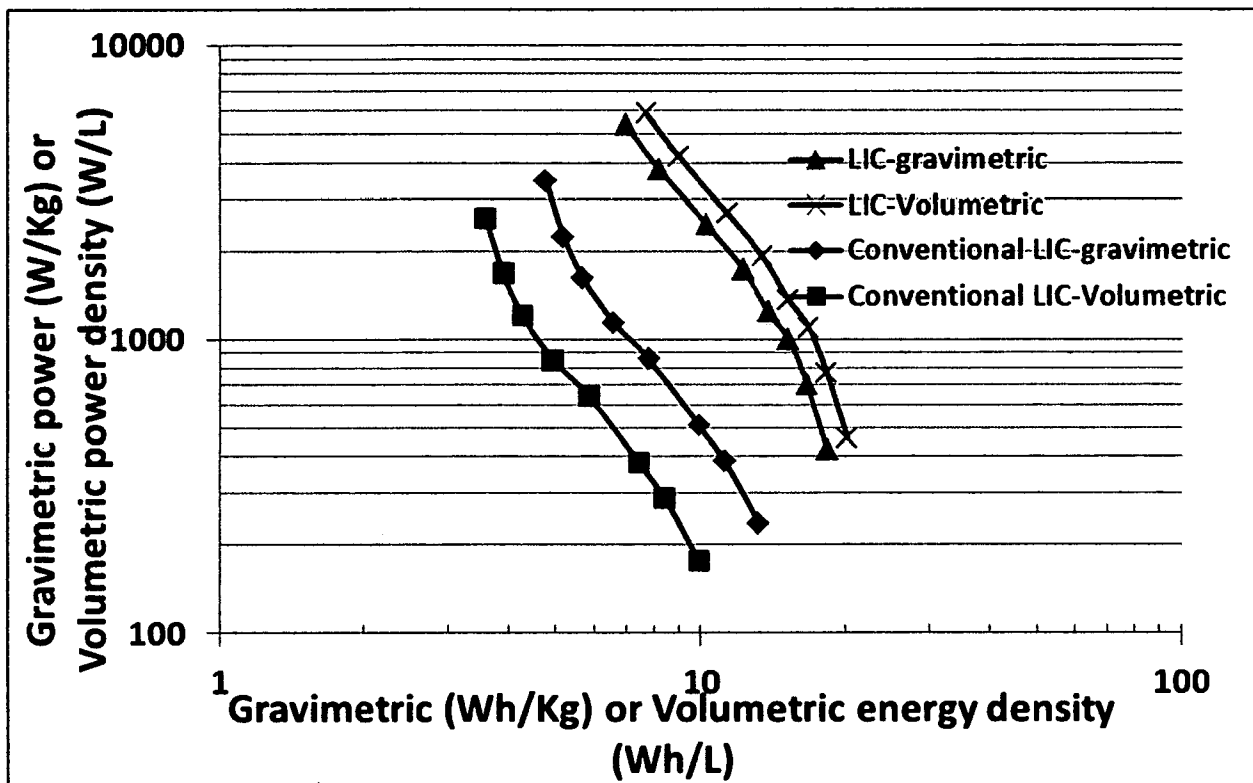
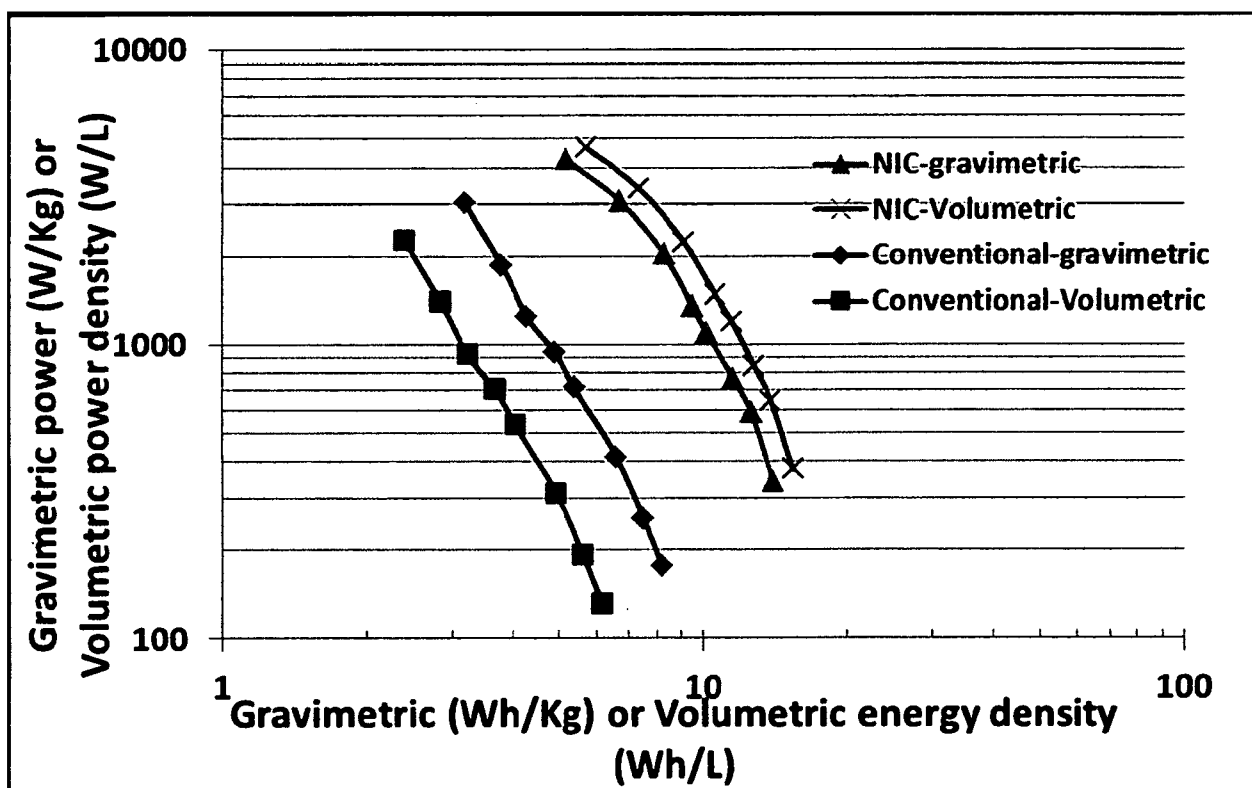
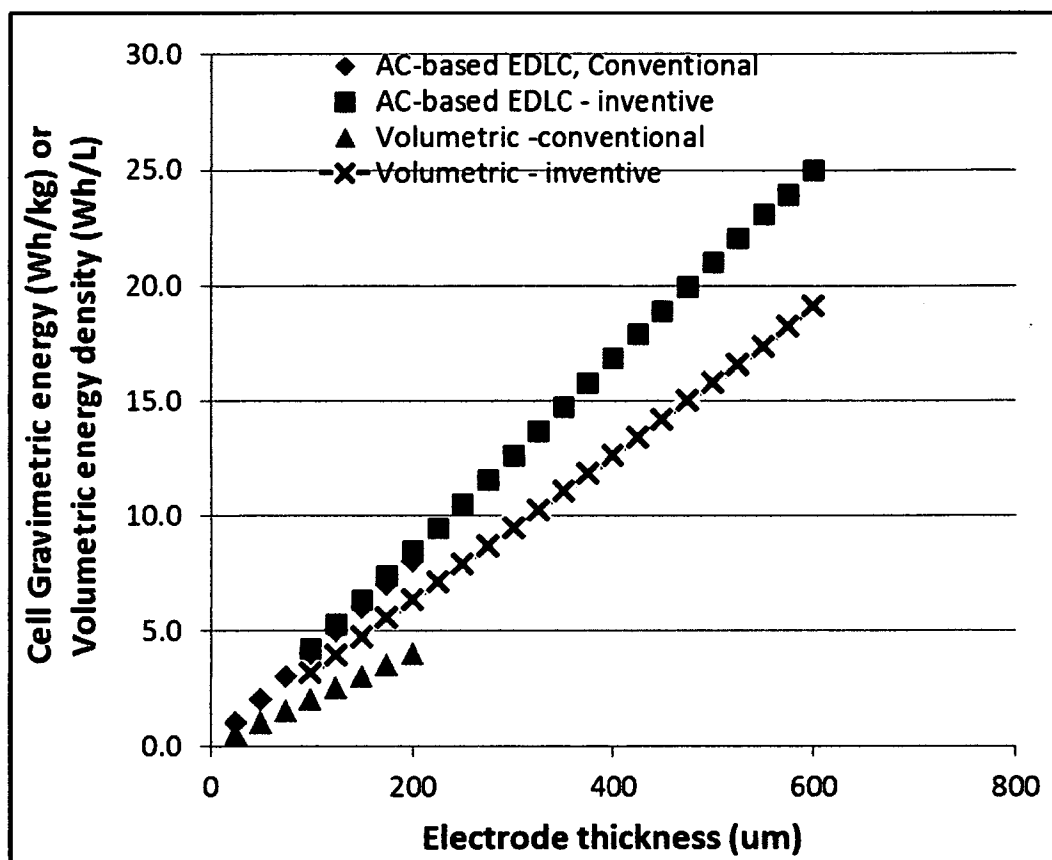
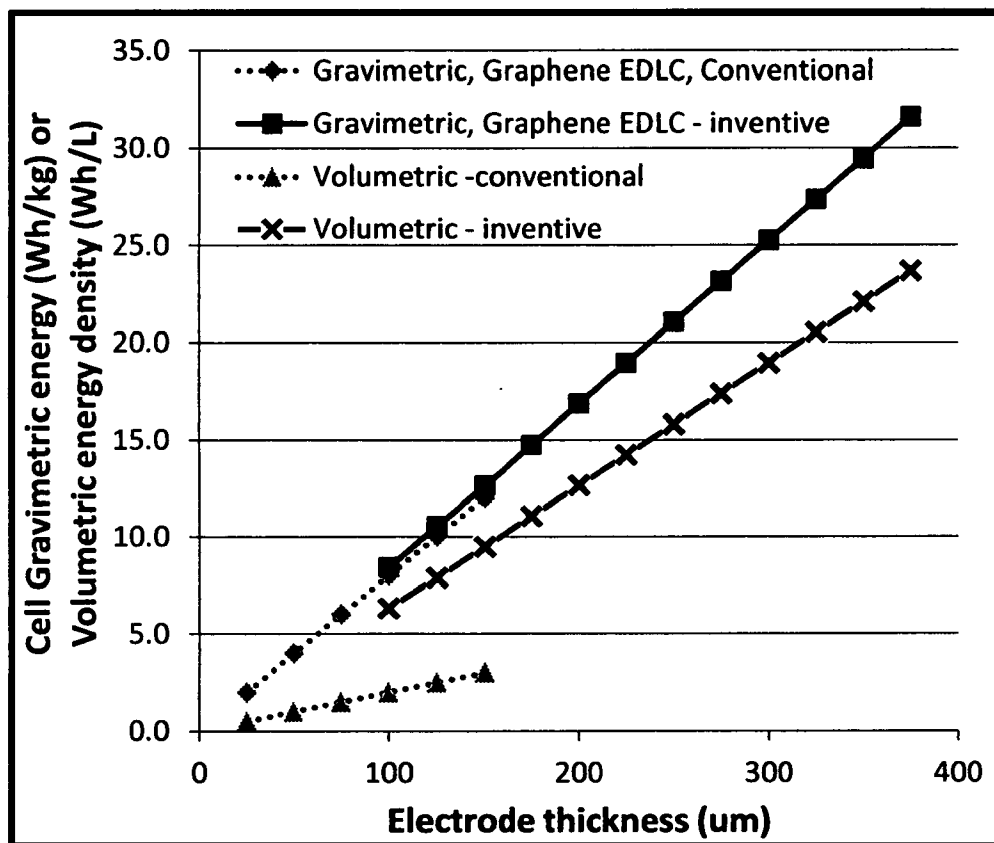


FIG. 7(A)

**FIG. 7(B)**

**FIG.8**

**FIG. 9**

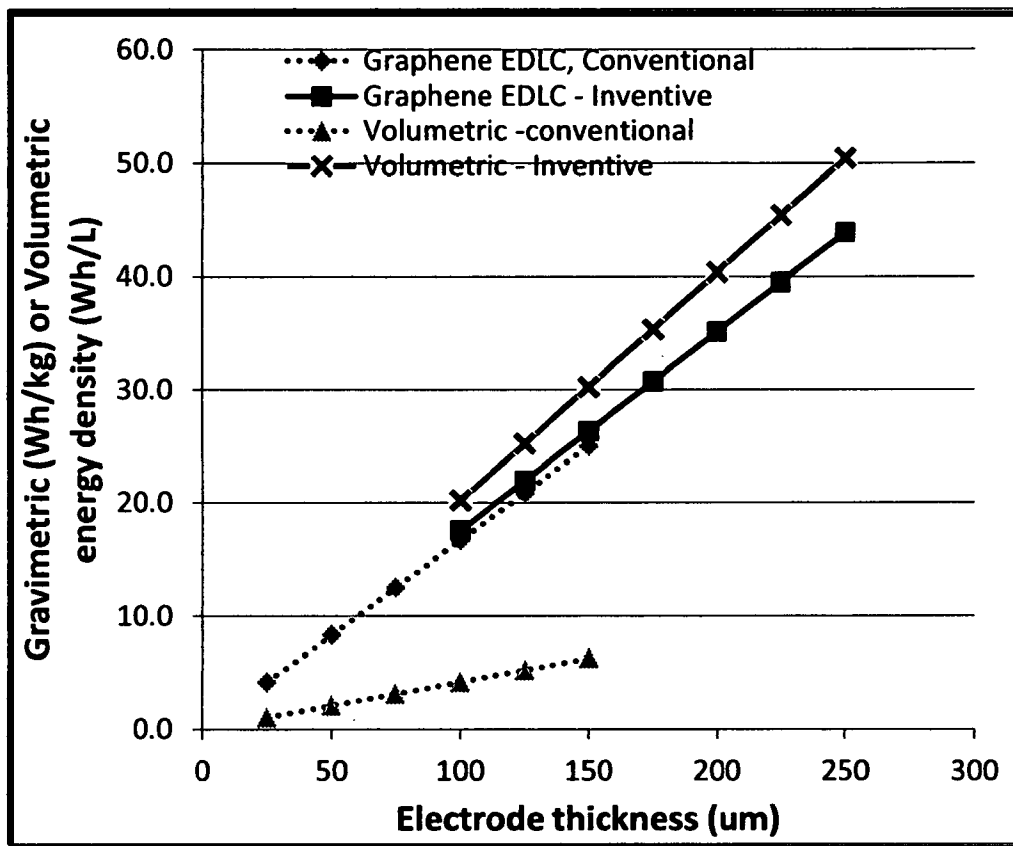
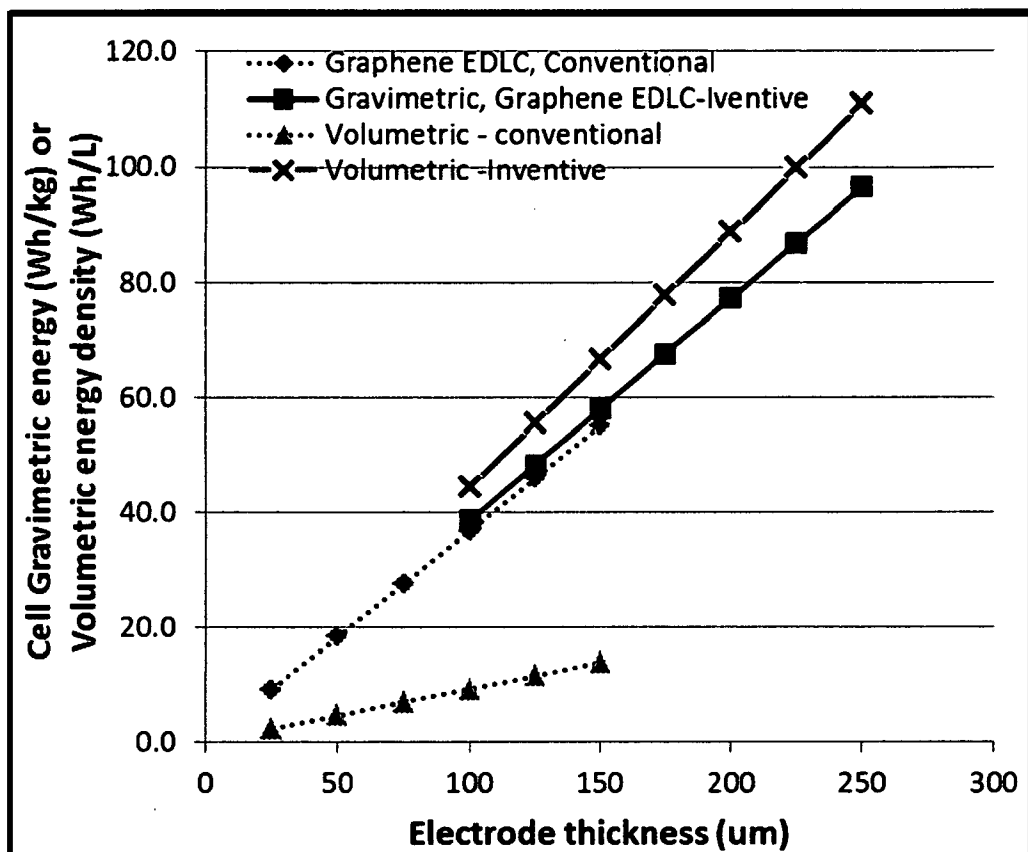
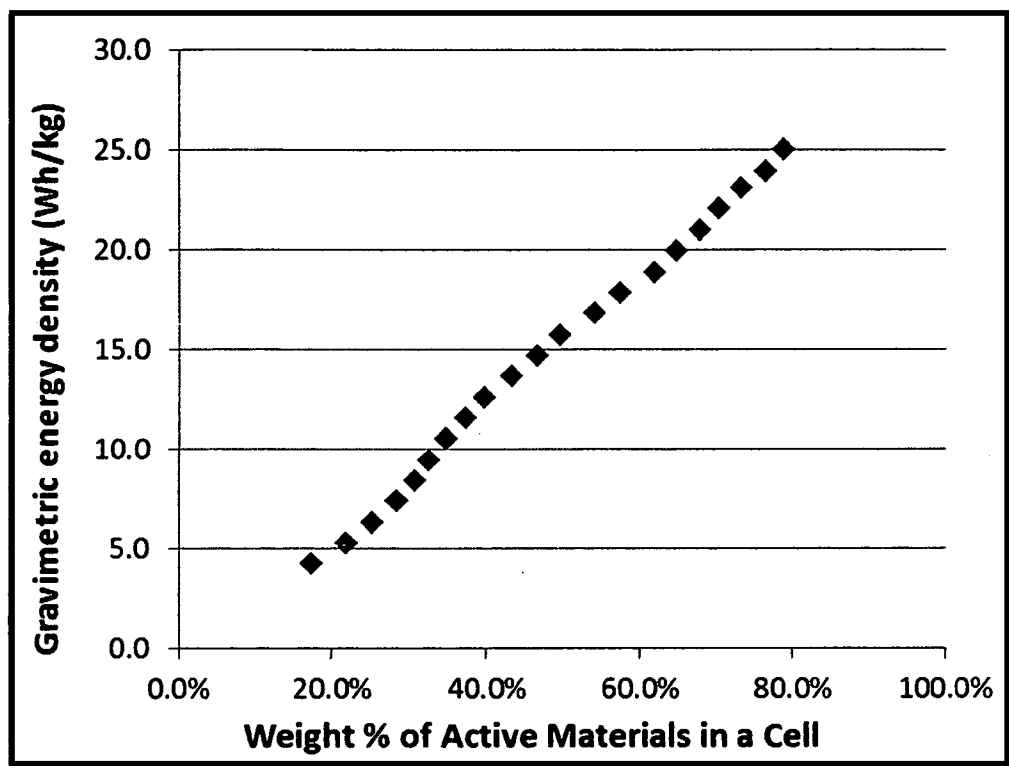


FIG. 10

**FIG. 11**

**FIG. 12**

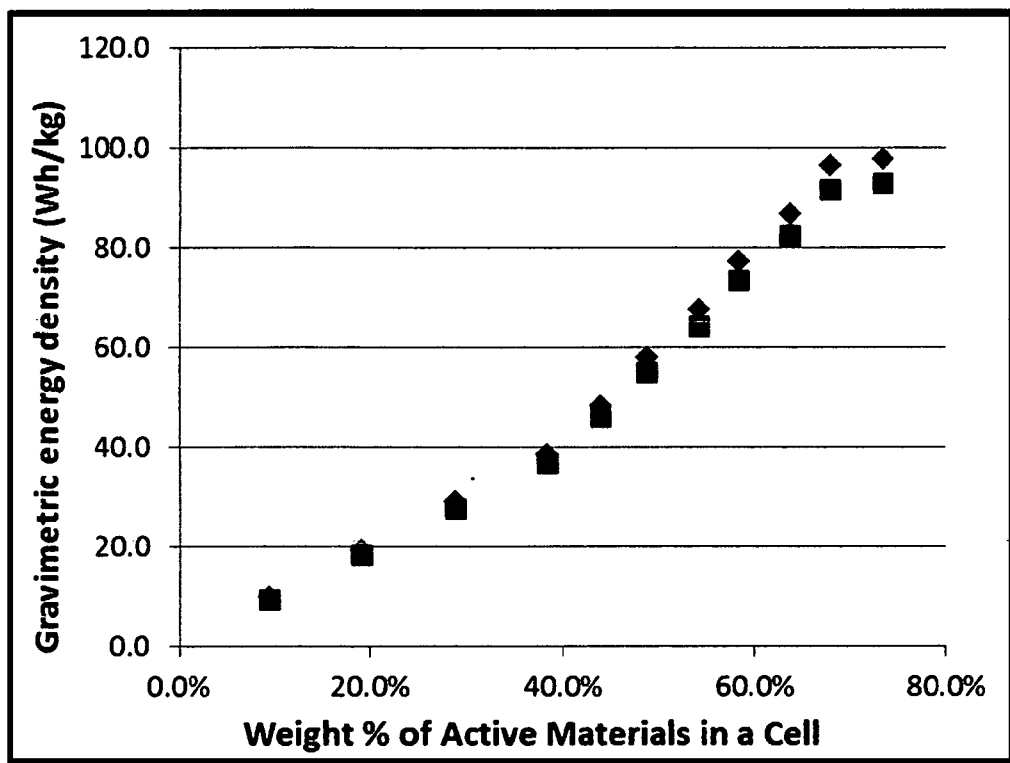
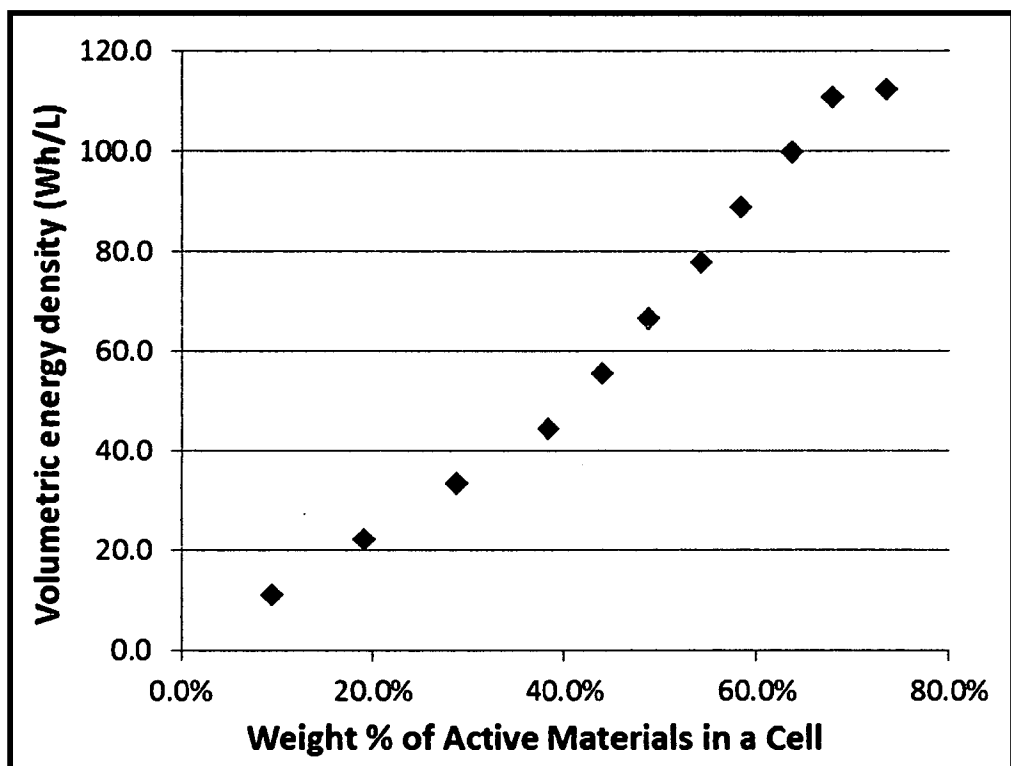


FIG. 13



INTERNATIONAL SEARCH REPORT

International application No.

PCT/US 16/62881

A. CLASSIFICATION OF SUBJECT MATTER

IPC(8) - H01L 21/44 (2017.01)

CPC - H01L 29/775, H01G 11/28, H01G 9/00, H01L 28/91

According to International Patent Classification (IPC) or to both national classification and IPC

B. FIELDS SEARCHED

Minimum documentation searched (classification system followed by classification symbols)
IPC(8)- H01L 21/44 (2016.01)
CPC- H01L 29/775, H01G 11/28, H01G 9/00, H01L 28/91

Documentation searched other than minimum documentation to the extent that such documents are included in the fields searched

Electronic data base consulted during the international search (name of data base and, where practicable, search terms used)
PatBase, Google Patents, Google Scholar (without Patents)

keywords: producing supercapacitor cell electrically conductive porous layers wet anode cathode

C. DOCUMENTS CONSIDERED TO BE RELEVANT

Category*	Citation of document, with indication, where appropriate, of the relevant passages	Relevant to claim No.
Y	US 2013/0162216 A1 (Zhamu et al.) 27 June 2013 (27.06.2013) Abstract, para [00124], para [00126], para [00127], para [00106], para [0077], para [00163], para [0061], para [0056], para [00235], para [00137], Figure 4A, Figure 5 and entire document	1-35
Y	US 2014/0030590 A1 (Wang et al.) 30 January 2014 (30.01.2014) Abstract, para [0080], para [00118], para [00128], para [00133], para [0022], para [00132] and entire document	1-35
A	US 2005/0175894 A1 (Visco et al.) 11 August 2005 (01.08.2005) Abstract, para [0012]-[0019]	1-35
A	US 7,623,340 B1 (Song et al.) 24 November 2009 (24.11.2009) Abstract,(Col 5 ln 60)-col 6 ln 35	1-35
P,X	US 9,437,372 B1 (Zhamu et al.) 6 September 2016 (06.09.2016) Abstract, col 7 -col 28	1-35
A	US 2012/0026643 A1 (Yu et al.) 2 February 2012 (02.02.2012) Abstract; para [0032]-[0041]	1-35

Further documents are listed in the continuation of Box C.

* Special categories of cited documents:

- "A" document defining the general state of the art which is not considered to be of particular relevance
- "E" earlier application or patent but published on or after the international filing date
- "L" document which may throw doubts on priority claim(s) or which is cited to establish the publication date of another citation or other special reason (as specified)
- "O" document referring to an oral disclosure, use, exhibition or other means
- "P" document published prior to the international filing date but later than the priority date claimed

- "T" later document published after the international filing date or priority date and not in conflict with the application but cited to understand the principle or theory underlying the invention
- "X" document of particular relevance; the claimed invention cannot be considered novel or cannot be considered to involve an inventive step when the document is taken alone
- "Y" document of particular relevance; the claimed invention cannot be considered to involve an inventive step when the document is combined with one or more other such documents, such combination being obvious to a person skilled in the art
- "&" document member of the same patent family

Date of the actual completion of the international search

19 January 2017

Date of mailing of the international search report

02 FEB 2017

Name and mailing address of the ISA/US

Mail Stop PCT, Attn: ISA/US, Commissioner for Patents
P.O. Box 1450, Alexandria, Virginia 22313-1450
Facsimile No. 571-273-8300

Authorized officer:

Lee W. Young

PCT Helpdesk: 571-272-4300
PCT OSP: 571-272-7774